AD-755 823

SMALL ROCKET INSTRUMENTATION FOR MEASUREMENTS OF INFRARED EMISSIONS-ASTROBEE D 30.205-3 AND ASTROBEE D 30.205-4

Larry L. Jensen, et al

Utah State University

Prepared for:

Air Force Cambridge Research Laboratories

November 1972

DISTRIBUTED BY:

NTIS

National Technical Information Service
U. S. DEPARTMENT OF COMMERCE
5285 Port Royal Road, Springfield Va. 22151

AFCRL 72-0691

space science laboratory

Small Rocket Instrumentation for Measurements of Infrared Emissions— Astrobee D 30.205-3 and Astrobee D 30.205-4

AD 758233

by

Larry L. Jensen, John C. Kemp, and Ronald J. Bell

SCIENTIFIC REPORT NO. 3

November 1972

Contract No. F19628-70-C-0302
Project No. 7663
Task No. 766303
Work Unit No. 76630301

Prepared for Air Force Cambridge Research Laboratories
Air Force Systems Command, United States Air Force
Bedford, Massachusetts 01730

Contract Monitor: James C. Ulwick
Ionospheric Physics Laboratory

This research was partially supported by the Defense Nuclear Agency.

Approved for public release; distribution unlimited.

UTAH STATE UNIVERSITY

CENTER FOR RESEARCH IN AERONOMY LOGAN, UTAH 84322

87

AFCRL-72-0691

SMALL ROCKET INSTRUMENTATION FOR MEASUREMENTS OF INFRARED EMISSIONS -- ASTROBEE D 30.205-3 AND ASTROBEE D 30.205-4

by

Larry L. Jensen, John C. Kemp, and Ronald J. Bell

Space Science Laboratory
Center for Research in Aeronomy
Utah State University
Logan, Utah 84322

Contract No. F19628-70-C-0302
Project No. 7663
Task No. 766303
Work Unit No. 76630301

Scientific Report No. 3

November 1972

Approved for public release; distribution unlimited.

Prepared for

Air Force Cambridge Research Laboratories
Air Force Systems Command
United States Air Force
Bedford, Massachusetts 01730

/c

Unclassified
Security Classification

DOCUMENT CONTROL DATA - R & D

(Security classification of title, body of abstract and indexing annotation must be entered when the overall report is classified)

1. ORIGINATING ACTIVITY (Corporate author) Space Science Laboratory Utah State University Logan, Utah 84322	2a. REPORT SECURITY CLASSIFICATION Unclassified 2b. GROUP

3. REPORT TITLE
SMALL ROCKET INSTRUMENTATION FOR MEASUREMENTS OF INFRARED EMISSIONS — ASTROBEE D 30.205-3 AND ASTROBEE D 30.205-4

4. DESCRIPTIVE NOTES (Type of report and inclusive dates)
Scientific Interim

5. AUTHOR(S) (First name, middle initial, last name)
Larry L. Jensen
John C. Kemp
Ronald J. Bell

6. REPORT DATE	7a. TOTAL NO. OF PAGES	7b. NO. OF REFS
November 1972	89	8

8a. CONTRACT OR GRANT NO. F19628-70-C-0302 b. PROJECT, Task, Work Unit Nos. 7663-03-01 c. DoD Element 62101F d. DoD Element 687663	9a. ORIGINATOR'S REPORT NUMBER(S) Scientific Report No. 3 9b. OTHER REPORT NO(S) (Any other numbers that may be assigned this report) AFCRL-72-0691

10. DISTRIBUTION STATEMENT
A-Approved for public release; distribution unlimited.

11. SUPPLEMENTARY NOTES TECH, OTHER	12. SPONSORING MILITARY ACTIVITY Air Force Cambridge Research Laboratories (LI) L. G. Hanscom Field Bedford, Massachusetts 01730

13. ABSTRACT

Two Astrobee D payloads, developed and instrumented at the Space Science Laboratory, Utah State University, under contract with the Air Force Cambridge Research Laboratories, were flown from Poker Flat, Alaska, as part of ICECAP 72 -- a continuing auroral measurements program. The first payload (30.205-3) contained a cooled, dual-channel radiometer which measured OH emissions in the 1.4 to 1.65 μ and 1.85 to 2.12 μ bands and was flown into a quiet nighttime sky with respect to OH enhancement. The second payload (30.205-4) contained a cooled, circular variable filter spectrometer which measured the infrared radiation spectrum between 1.65 and 5.3 μ and was launched into a medium bright auroral display accompanied by indicated OH enhancement.

All systems functioned properly during both flights and preliminary analysis indicates that good data were received. The flights also provided certification for two new instruments and generally furthered small rocket measurements techniques.

Details of illustrations in this document may be better studied on microfiche

ia

DD FORM 1 NOV 65 1473

Unclassified
Security Classification

14 KEY WORDS	LINK A		LINK B		LINK C	
	ROLE	WT	ROLE	WT	ROLE	WT
ICECAP 72						
Auroral measurements						
Infrared measurements						
Astrobee D instrumentation						
OH infrared measurements						
Infrared spectrum						

LIST OF CONTRIBUTORS -- SCIENTISTS AND ENGINEERS

K. D. Baker -- Principal Investigator

D. J. Baker
R. H. Bishop
D. A. Burt
D. G. Frodsham
L. L. Jensen
J. C. Kemp
C. L. Wyatt

RELATED CONTRACTS AND PUBLICATIONS

F19628-67-C-0275

Baker, K. D and G. D. Allred, Arcas rocket instrumentation development for mesospheric measurements, *USU Scientific Report No. 1, AFCRL - ,* 68 pp., Contract F19628-70-C-0302, Space Science Laboratory, Utah State University, Logan, June 1972.

Baker, K. D., D. A. Burt, L. C. Howlett, and G. D. Allred, Rocket instrumentation for the study of a Polar Cap Absorption Event -- PCA 69, *UARL Final Report, AFCRL 70-0251,* 270 pp., Contract F19628-67-C-0275, Upper Air Research Laboratories, University of Utah, Salt Lake City, April 1970.

Bishop, R. H., *Antenna Impedance in the Lower Ionosphere,* 152 pp., Space Science Laboratory, Utah State University, Logan, September 1970.

Burt, D. A. and G. D. Allred, Rocket instrumentation for PCA measurements -- Black Brant 17.757, *UARL Scientific Report No. 4, AFCRL 70-0196,* 79 pp., Contract F19628-67-C-0275, Upper Air Research Laboratory, University of Utah, Salt Lake City, March 1970.

Burt, D. A., Rocket instrumentation for PCA measurements -- Black Brant 17.750 and 17.751, *UARL Scientific Report No. 3, AFCRL 69-0282,* 79 pp., Contract F19628-67-C-0275, Upper Air Research Laboratory, University of Utah, Salt Lake City, June 1969.

PREFACE

At Utah State University a number of individuals had specific responsibilities for various phases of this project:

Principal Investigator and Project Scientist	K. D. Baker
Project Engineer	L. L. Jensen
Payload Fabrication	D. D. Olsen M. E. Taylor
Field Operations	L. L. Jensen J. C. Kemp
Cooled, Dual-channel Radiometer	J. C. Kemp
CVF Spectrometer	J. C. Kemp
Documentation	R. J. Bell D. A. Brookshier R. M. Fowler

TABLE OF CONTENTS

LIST OF ILLUSTRATIONS

Preceding page blank

LIST OF ILLUSTRATIONS (cont.)

LIST OF TABLES

INTRODUCTION

During March 1972 the ICECAP 72 infrared measurements program was conducted at the Poker Flat Research Range near Fairbanks, Alaska. This program consisted of coordinated rocketborne and ground-based measurements directed primarily toward accumulating data pertinent to the classification and understanding of atmospheric infrared emissions associated with auroral activity. The interest in auroral infrared measurements precipitates from recent observations of these phenomena, speculation as to extent of their effect upon our nation's defense systems, and the use of these emissions to help in understanding the controlling atmospheric processes. This understanding will in turn facilitate the proper development of computer codes that will allow prediction of atmospheric effects under various stimuli. The infrared emissions are not restricted to a single radiating species but several atmospheric constituents seem to be involved. *Noxon* [1970] and *Megill, et al.*, [1970] reported enhanced infrared radiation in conjunction with aurora from a metastable state of oxygen, $O_2(^1\Delta_g)$. *Zipf, et al.*, [1970] reported greatly enhanced nitric oxide (NO) concentrations in at least some auroras which would result in rather large infrared emissions. As a result of measurements from a series of aircraft flights into the northern auroral zone, *Stair, et al.*, [1971] report hydroxyl (OH) emissions that increased by a factor of 2 or 3 in conjunction with, but not spatially correlated with, visible auroral activity. Enhancements of the various atmospheric emissions as noted by these scientists must be accompanied by significant changes in the atmospheric chemistry of the region involved, which to date are not fully understood. The ICECAP 72 measurements program was designed and conducted to further this understanding on a broad basis.

In the initial ICECAP 72 planning, one important facet of the total program was the investigation of atmospheric OH chemistry through its associated infrared emissions. Accomplishment of this objective involved the use of two Astrobee D rockets, each instrumented with a cooled dual-channel radiometer to make direct *in situ* measurements of

OH radiations at two different wavelength regions. The rocket launches would be controlled by monitoring the OH emissions using aircraftborne instruments. The rockets would fly through the region viewed by the aircraft instruments, yielding a vertical profile of the OH emissions which could be used to interpret the aircraft measurements. It was envisioned that one rocket would be flown during "quiet" or normal background OH conditions and the other would be flown when the aircraft measurements indicated an enhancement of the OH emissions. Ground-based measurements would be used to monitor and classify the general auroral conditions at the time the aircraft and rocket measurements were being performed.

The ICECAP 72 measurements program also included a Black Brant V rocket with a complex array of instruments to make measurements of incoming auroral particle fluxes, ionospheric effects, and visible and infrared emissions associated with the aurora (*Burt, et al.*, 1972). Included in the array of instruments were cryogenically cooled radiometers measuring infrared emissions in rather narrow fixed wavelength intervals between 1.6 and 5.5 μ in order to determine the emissions and concentrations of important species such as nitric oxide, hydroxyl and carbon dioxide. Interpretation of these measurements would be facilitated by data from a cooled, circular variable filter (CVF) spectrometer which would scan the short wave infrared spectrum from about 1.5 to 5.5 μ. As the program progressed, it became apparent through mechanical and physical constraints that the CVF spectrometer could not be included in the Black Brant payload. At that point it was decided that the dual-channel radiometer would be removed from one of the Astrobee D payloads and the CVF spectrometer flown in its place. By flying the Astrobee D payload simultaneously with the Black Brant, the spectrometer would still provide supporting spectral measurements for the Black Brant radiometer measurements.

A further modification of the ICECAP 72 plan was necessitated when the aircraft measurements originally called for could not be made (aircraft scheduling problems) and the Astrobee D containing the CVF spectrometer could not be flown simultaneously with the Black Brant

(operational problems). As originally planned, one Astrobee D with a cooled, dual-channel radiometer was flown into quiet OH conditions as determined by the aircraft instrument (a dual-channel lead sulfide radiometer) which was used on the ground at the launch site. The CVF spectrometer was flown into a moderately bright auroral display to flight test the instrument and provide preliminary measurements of short wave infrared emissions in an aurora. Although changed in manner of execution, much of the original philosophy and objectives associated with the Astrobee D payloads remained. These objectives bore directly 1) upon the measurements themselves, and 2) upon the state of the art of ionospheric measurements techniques generally.

The Astrobee D payloads measured short wave infrared emissions in the 1.4 to 5.3 μ region which contains radiation from prominent infrared emitters such as NO, OH, CO_2 and NO^+. By identifying the various species, their concentrations and spacial extents through the wavelength and strength of their emissions, the aurora can be characterized as an infrared emitter. Such knowledge will lead to increased understanding of the chemistry of the excited region.

The state of the art of ionospheric measurements was advanced by the implementation of new techniques (on two fronts) for rocketborne measurements, i.e., cooling the measuring device to low temperatures via the application of a cryogen (liquid nitrogen), and miniaturizing the instruments to enable the use of small rockets as the vehicles for transporting them to ionospheric altitudes. Measurements of selected infrared wavelengths of relatively low magnitude can be more accurate if radiations from the instrument itself are eliminated or greatly reduced to prevent them from contaminating or masking the radiations emanating from the desired source. For this experimental application each Astrobee D contained instrumentation cooled to liquid nitrogen temperatures (77°K) to reduce instrument background radiation to acceptable levels. The Astrobee D vehicles categorically can be classified as small rockets by ionospheric research standards and are routinely used for meteorological measurements. This was the initial application by the Air Force Cambridge Research Laboratories/Utah State

University of this vehicle for ionospheric research. The advantages of small rocket vehicles have been proven in other research programs [*Baker* and *Allred*, 1972; *Burt*, *et al.*, 1972] and include reduced costs, ease of handling, and reduced technical support requirements (both facilities and personnel). They provide an ideal platform for testing new instruments by allowing the instruments to be evaluated individually rather than as a part of the complex payloads typically employed on larger rockets and by relating the flight objectives to the specific instrument rather than to a complex grouping.

The payload used to measure "quiet" OH emissions (30.205-3) was instrumented with the cooled, dual-channel radiometer which measured infrared radiation in the 1.4 to 1.65 and 1.85 to 2.12-μ bands. These bands are the result of emission through relaxation from the excited vibrational states of OH in the $\Delta v = 2$ series. The 1.4 to 1.65-μ channel will include transitions related to the low vibrational levels of 2-0 to 6-4. The 1.85 to 2.12-μ channel will include transitions related to the higher vibrational energy levels of 7-5 to 9-7. The principle excitation mechanism producing excited vibrational states of OH is

$$H + O_3 \longrightarrow OH^* + O_2$$

where * indicates an excited state of OH. This process, known as the ozone process, yields excited OH states up to and including the ninth vibrational level. A possible secondary source is

$$O + HO_2 \longrightarrow OH^* + O_2$$

and yields excited OH states only up to and including the sixth vibrational levels. By comparing the outputs of the two radiometer channels, the relative importance of the ozone and secondary processes can be evaluated.

The other payload (30.205-4) contained the cooled circular variable filter (CVF) spectrometer and measured IR radiation in the 1.65 to 5.3 μ region during auroral conditions. The CVF spectrometer contains an interference filter that is constructed by varying the thickness of the interference material with angular displacement such that as the

filter is rotated, the spectral region of interest is *linearly scanned*. In addition to OH emissions, the wavelength region scanned by the spectrometer includes other important species such as NO, NO^+, and CO_2. The spectral data from this instrument can be invaluable in unscrambling overlapping emission bands. The remainder of this report describes the technical details of these two Astrobee D payloads.

INSTRUMENTATION

General Payload Description

The Astrobee D payloads consisted of instrumentation as noted in Table 1. In order to accomplish the measurements objectives, the payloads were mated to the rocket and the instruments were cooled with liquid nitrogen through openings provided in the payload skin. Umbilical connections were provided so the instrument and payload functions could be tested and monitored up to the moment of liftoff. The payloads were launched when proper atmospheric conditions occurred (as determined by the project scientsts). When the appropriate altitudes

TABLE 1

Astrobee D 30.205-3 and 30.205-4 Payloads

Rocket	Launch Date/Time	Instrument	Measurements
30.205-3	6 Mar 72 0214 Local	Cooled dual-channel radiometer	OH (1.4 - 1.65 μ) (1.85 - 2.12 μ)
		Magnetometer	Magnetic aspect
		Baroswitch	Trajectcry check points
30.205-4	9 Mar 72 0052 Local	Circular variable filter spectrometer	IR emission spectra (1.65 - 5.3 μ)
		Magnetometer	Magnetic aspect
		Baroswitch	Trajectory check points

were achieved, the measuring instruments were exposed and the measurements commenced. Data from the payloads were telemetered to the ground station where they were displayed in real time and were recorded for future analysis.

Both payloads were designed with the prime instrument oriented to view directly ahead with respect to the vehicle major axis with fields of view as shown in Figure 1. Supporting instrumentation included a magnetometer to provide magnetic aspect and a baroswitch to give an indication of the rocket's passage through an altitude of 75,000 ft during ascent and descent.

Vehicle Description

The Astrobee D is a relatively new rocket designed for meteorological investigations. This is the first time this model has been used in conjunction with a Space Science Laboratory experiment. It incorporates a dual thrust, solid propellant motor, which provides moderately rapid acceleration at liftoff (to minimize the effects of wind), and a long sustain time (to achieve a "soft ride") with moderate burnout Mach numbers at high altitudes. When launched at sea level, the Astrobee D is capable of lifting a 10 pound payload to altitudes of approximately 130 km, or a 30 pound payload to approximately 90 km. The rocket is small enough that it can be easily handled in the field and may be fired from a variety of launchers making it a versatile vehicle for scientific investigations. Figure 2 shows the major dimensions of the Astrobee D rocket.

Nosetip Separation

The instruments carried aboard the Astrobee D rockets were designed to make measurements in the altitude region of from 50 to 100 km, and to look forward with respect to the vehicle major axis. Therefore, a protective nose cone was provided which would make the payload aerodynamically stable and protect it during passage through the dense lower atmosphere. Since the instruments were also to be cooled, a "cold cover"

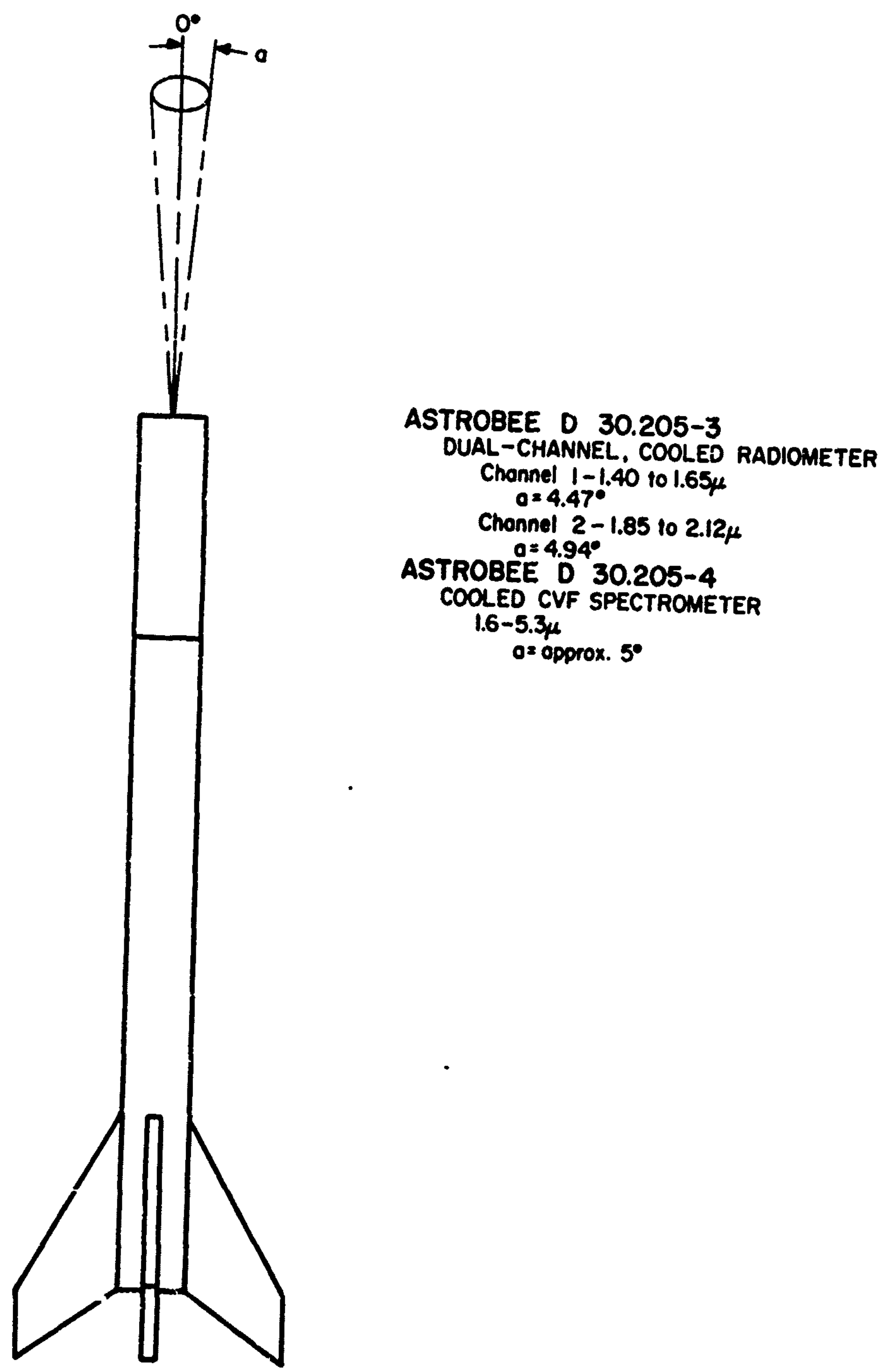

Figure 1. Astrobee D 30.205-3 and Astrobee D 30.205-4 Fields of View.

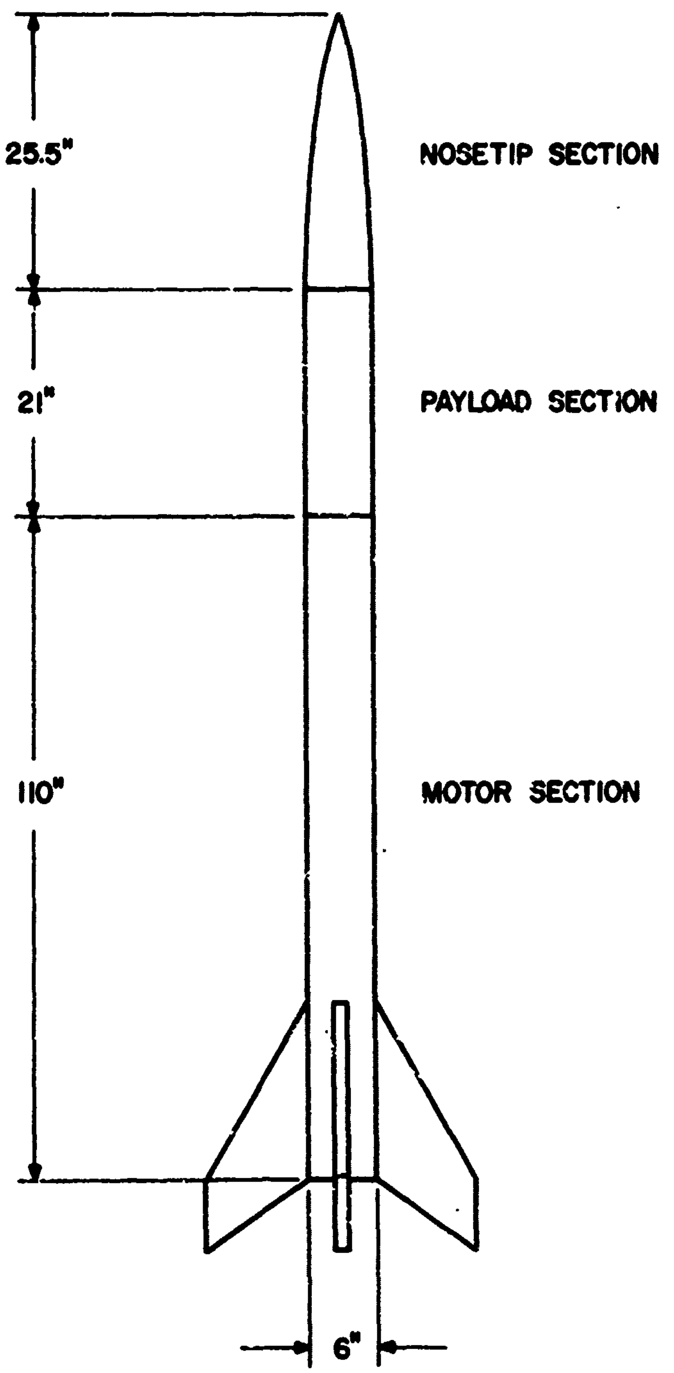

Figure 2. Astrobee D Major Dimensions

was provided and the optical compartment was evacuated prior to flight to keep the optics from frosting while in the dense lower atmosphere. Both of the above requirements were fulfilled by designing a nosetip which would separate at the appropriate altitude, removing the cold cover and exposing the instrument so measurements could be made.

The nose section is a clamshell-type assembly consisting of two halves constructed as shown in Figure 3. The halves are held together by a pin arrangement at the top and by a brass bolt located in the lower part of the nose section. The instrument cold cover is connected to the bottom of a piston and compressed spring arrangement, and is held in position over the front of the instrument by a brass bolt. The bolt passes through a guillotine which is connected to the separation timer. A nonrigid attachment to the cold cover is used so that integrity of the vacuum seal to the instrument is not disturbed by movement of the nose section.

Figure 4 is a graphic representation of the nosetip separation. At a preset time, the guillotine severs the piston holding bolt, allowing the compressed spring to expand, pushing the piston forward and pulling the cold cover off the instrument. (A partial vacuum existing on both sides of the cover allows easy removal at this time.) When the piston has traveled a sufficient distance to raise the cover above the detectors, a small microswitch is activated by the piston. The switch completes a second guillotine firing circuit. The second guillotine then shears the brass bolt holding the nose section together. The force of the guillotine action on the brass bolt imparts an initial horizontal movement to the nose-section halves. The nose section separates at the aft end first, being held momentarily by the pin arrangement at the front, and complete separation is accomplished by the centrifugal force developed by the rocket spin.

The electronic circuitry contained in the nose section provides the timing sequence to separate the payload nose section, and is completely independent of the remaining payload circuitry. The nose section contains its own battery, primary and secondary timing circuits, and pyrotechnic devices. Figure 5 is a block diagram of the primary

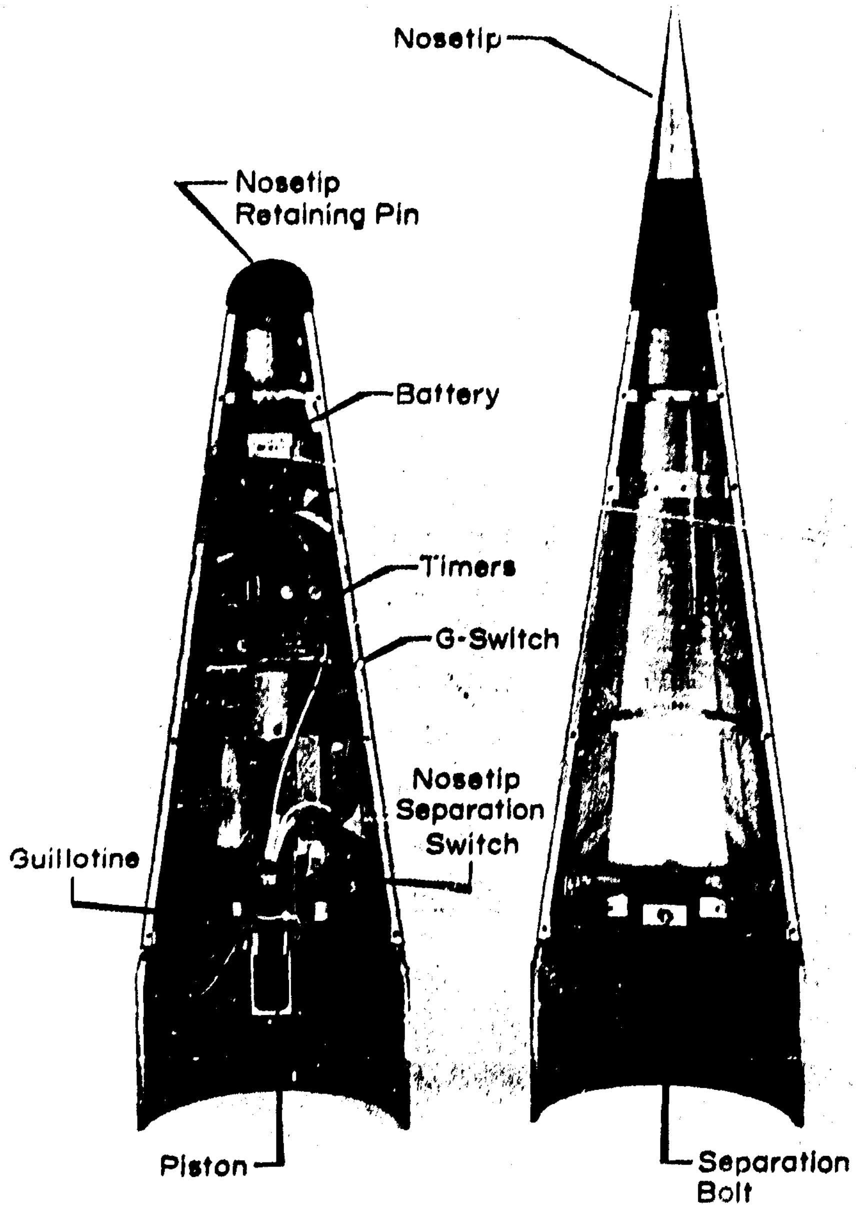

Figure 3. Nose Section Construction

and secondary timing circuits used to fire the first guillotine. As shown in the block diagram of Figure 5, operation of the primary timer commences with the momentary closure of the acceleration switch at rocket launch. The timer circuitry output is connected to the cold cover guillotine through a baroswitch (75,000 ft ± 3,000 ft) which normally closes during the primary timing interval. When the timing cycle is completed, an electrical impulse is sent to the guillotine attached to the cold cover piston. Closure of the baroswitch (at 75,000 ft ± 3,000 ft) starts a secondary timing circuit which provides a backup signal should the primary timer fail to fire the guillotine. In the event that the primary timer is activated and the baroswitch has not closed, an automatic reset circuit recycles the primary timer and the system is ready for use again. The secondary circuit is activated only by the closure of the baroswitch and, therefore, requires no reset circuitry.

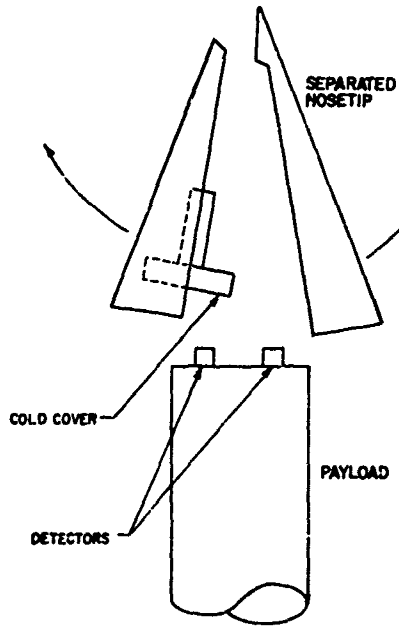

Figure 4. Nosetip separation.

The nose section separation is timed to occur at 50 km. A predicted height versus time trajectory was computed and the desired times determined. The primary and secondary timer settings for each payload are given in Table 2. In order to monitor the nosetip separation from the payload section, a microswitch was installed in the main payload which, with its related circuitry, provided a four volt output with the nosetip in place and a one volt output when the nosetip was removed. Schematic diagrams of the nosetip separation electronics are shown in Figures 6 and 7.

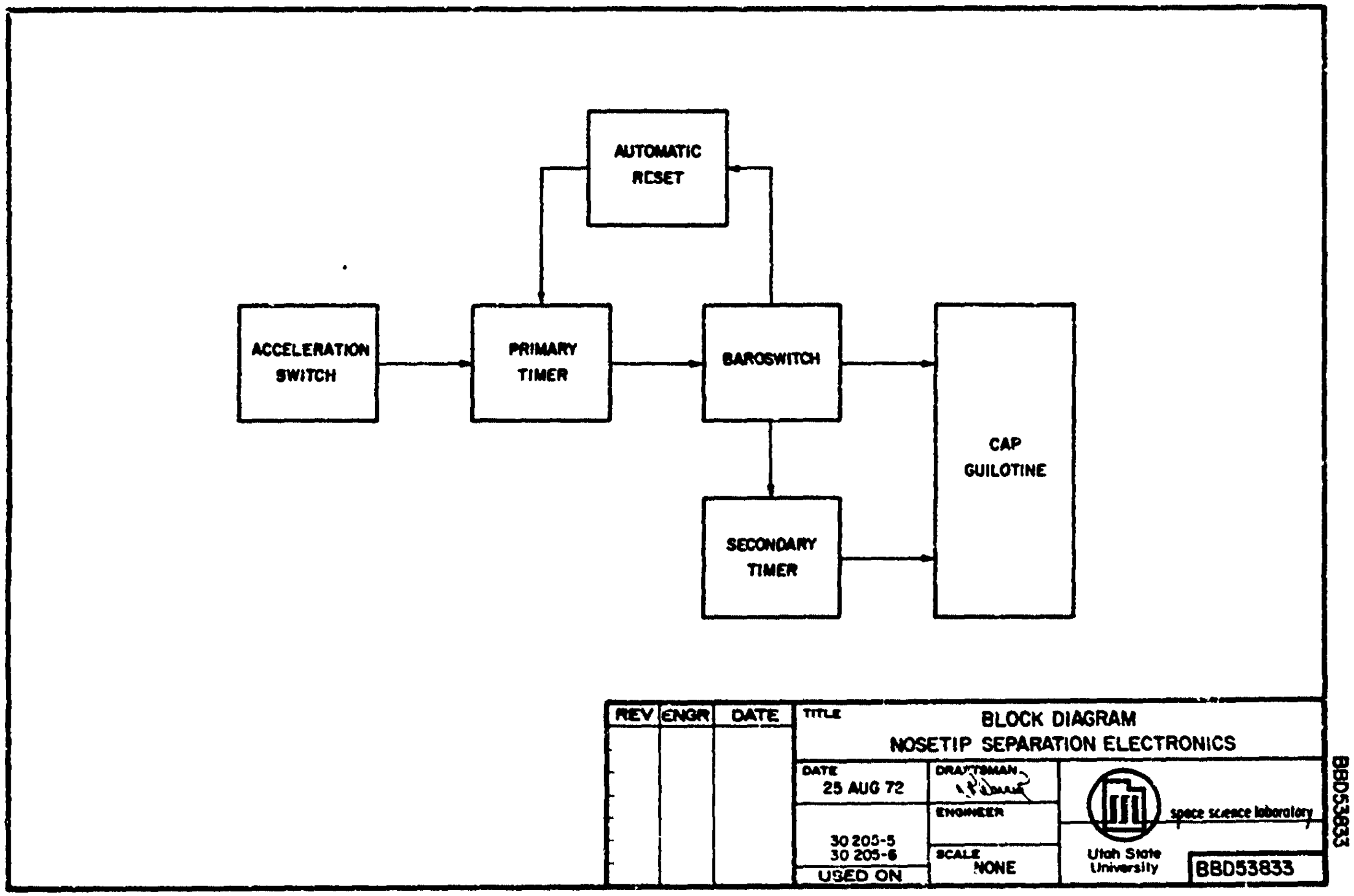

Figure 5. Nosetip separation electronics block diagram.

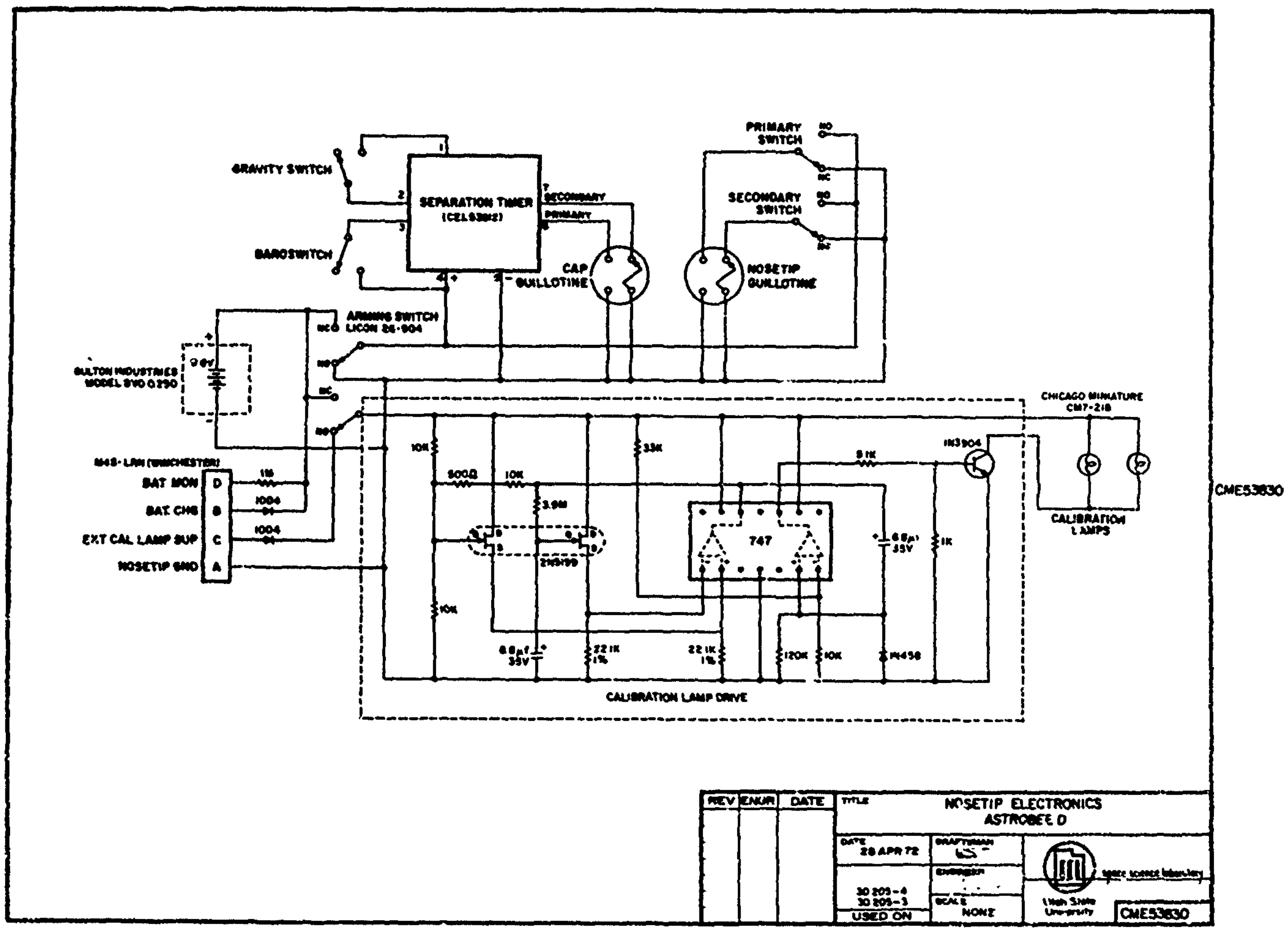

Figure 6. Nosetip electronics.

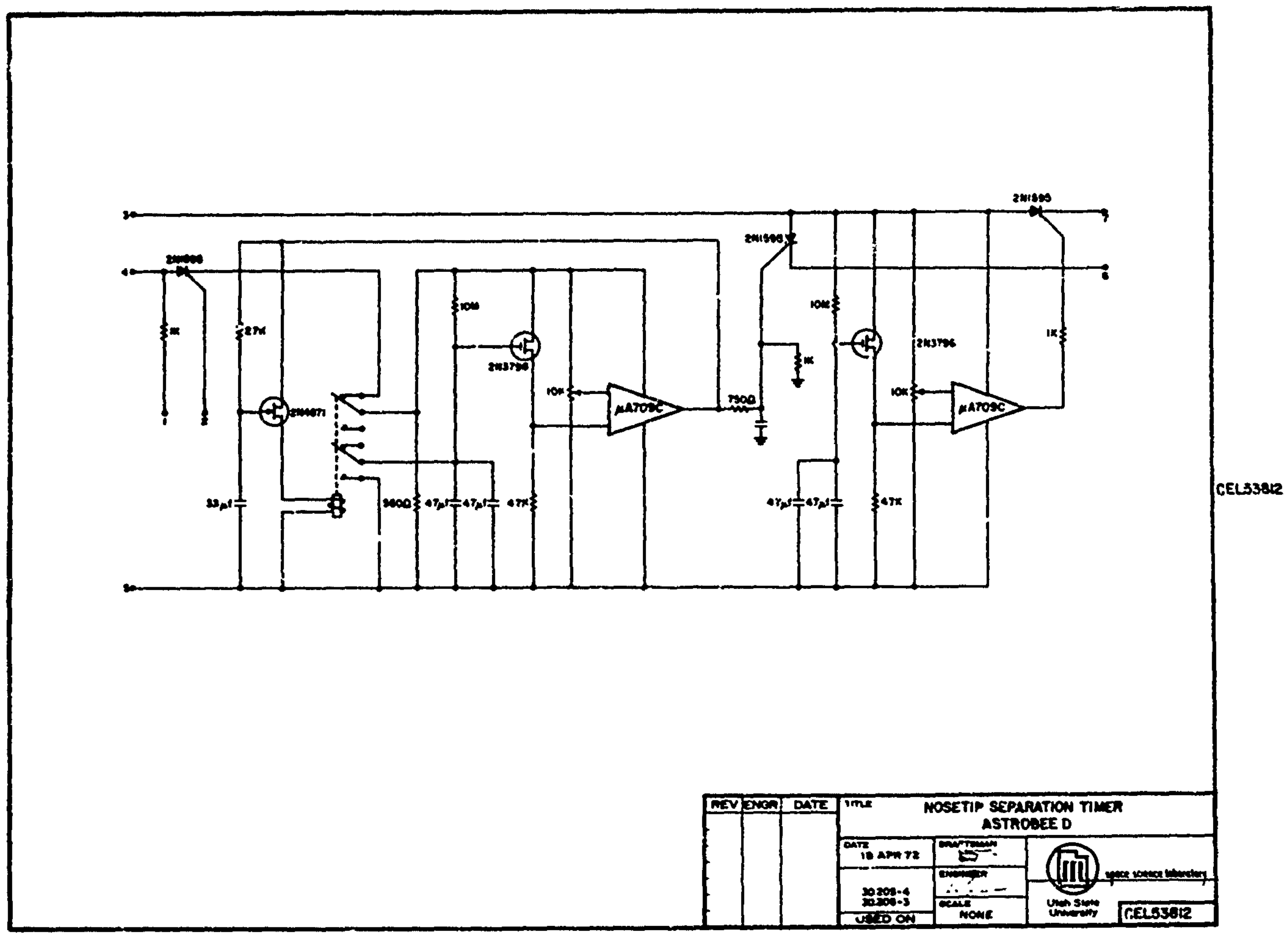

Figure 7. Nosetip separation timer electronics.

TABLE 2

Astrobee D Payload Timer Settings

Vehicle and Payload	Primary Timer Settings		Secondary Timer Settings*	
	Calculated	Actual**	Calculated	Actual**
A30-205-5 NR-3 Radiometer	56 sec	52.9	32 sec	
A30-205-6 NS-1 Spectrometer	53 sec	49.6	31 sec	

*Seconds after baroswitch closure (75,000 ft ± 3,000 ft)
**Time measured during flight

Cooled, Dual Channel Radiometer, NR-3-1 (Astrobee D 30.205-3)

The model NR-3-1 dual channel radiometer has two independent measurement channels mounted in a single dewar and using a common motor driven chopper. Figure 8 is a cutaway view of the NR-3-1 instrument showing the major components. The unit consists of a cryogenic vessel with a cold, optical compartment on the fore end and an electronics compartment on the aft end. Tubes extend through the liquid nitrogen vessel, permitting connection from the electronics compartment to the optical compartment of the electrical conductors and a motor drive shaft. The baffles, lenses, filters, detectors, source followers, preamplifiers, and a motor driven chopper are located in the cold optics compartment. The electronics compartment contains the chopper motor, reference generator, and signal conditioning electronics. The sealed unit is shown pictorially in Figure 9.

The cryogenic system is shown in the cutaway view of Figure 10. Liquid nitrogen (77°K) is used to cool the optics compartment and mount to reduce infrared emissions from the instrument itself. An absolute pressure relief valve is provided which maintains a constant pressure (18 psi) in the liquid nitrogen vessel, thereby protecting the dewar from damage by excessive pressure and preventing the liquid nitrogen from freezing through exposure to a vacuum. Because of the low temp-

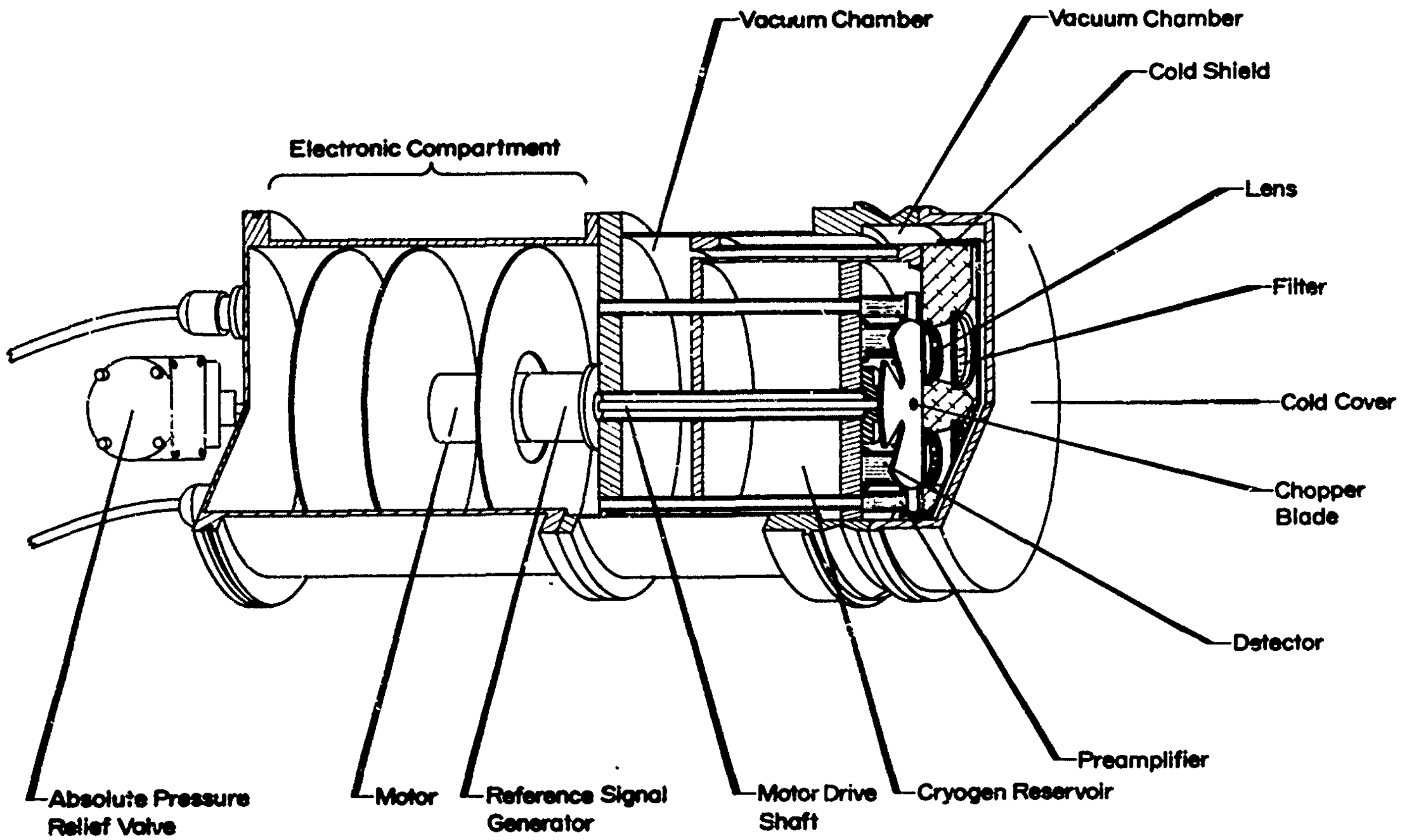

Figure 8. NR-3-1 cross section.

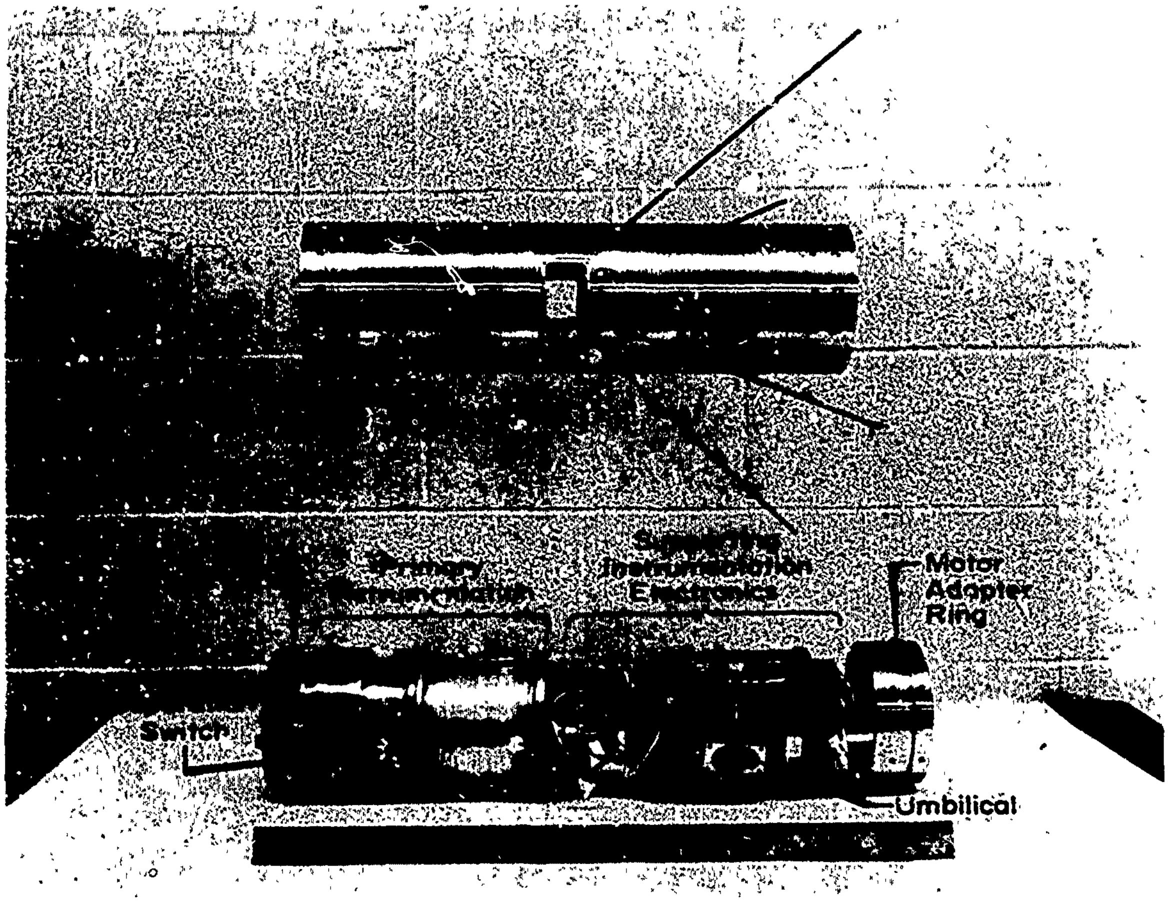

Figure 9. Astrobee D 30.205-3 payload.

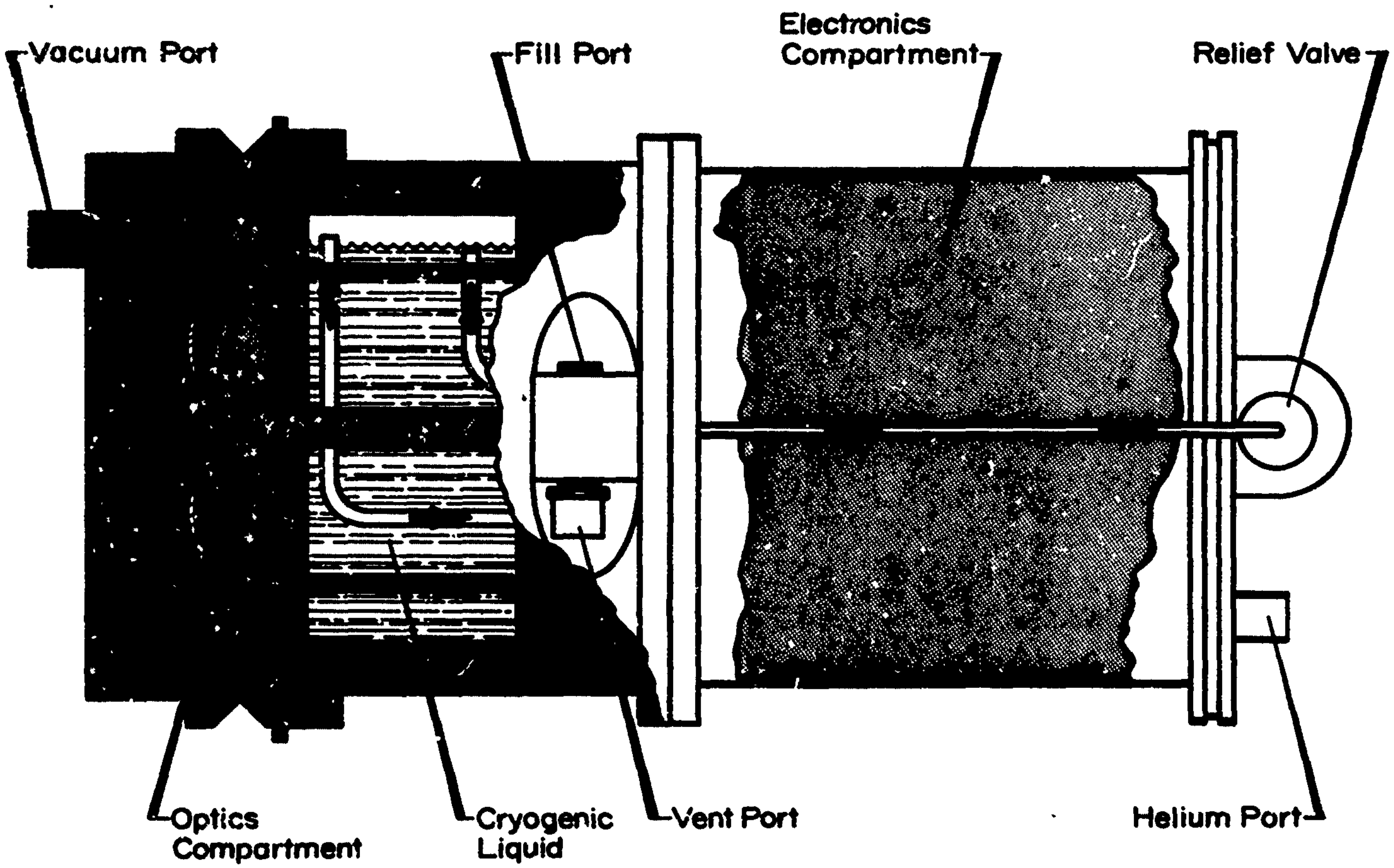

Figure 10. Cutaway View of Cryogenic System

eratures involved, indium O rings are used to seal the optics compartment since rubber would freeze. Special springs are used to maintain a constant pressure on the O rings as the dewar is cooled and warmed.

The filling and cooling process is initiated by evacuating the electronics and optics compartments to eliminate moisture-laden air which would cause frost buildup on the optical components. These compartments are then backfilled to approximately $\frac{1}{3}$ atmosphere with dry helium gas which also acts as a heat conductor to cool the optics components and motor. After leak testing the helium chambers, the cold cover is attached and the insulating vacuum is provided by evacuation. The liquid nitrogen vessel is filled using low pressure until the liquid nitrogen starts to escape from the vent. To achieve thermal equilibrium within the system, it is necessary to refill the liquid nitrogen vessel at least three times, waiting 15 to 20 minutes between each filling. Much of the liquid nitrogen is boiled away as heat is absorbed from the dewar during the cooling process, thereby necessitating the three refills. After the filling is completed, the vent and fill ports are plugged and the unit is ready to fly.

Figure 11 is a block diagram of the NR-3 system. As shown in the block diagram, incoming radiation is filtered to provide measurement of the desired wavelength. A coated silicon lens is used to focus the incident radiation on the detector. Prior to being detected, the radiation passes through a four-bladed rotating chopper yielding an alternating signal of 533 Hz. This provides a high signal to noise ratio in the system.

The photovoltiac infrared detector is an indium antimonide PN junction mounted on a Kovar base. At room temperature it has very low resistance (less than 100 ohms), but as the detector is cooled to 77°K its impedance increases to greater than one megohm. The increased impedance results in a high detectivity (D^*) since D^* is inversely proportional to the noise equivalent power (NEP) and is therefore proportional to the input impedance. The signal from the detector is coupled to the preamplifier using a cooled, dual source follower. This pro-

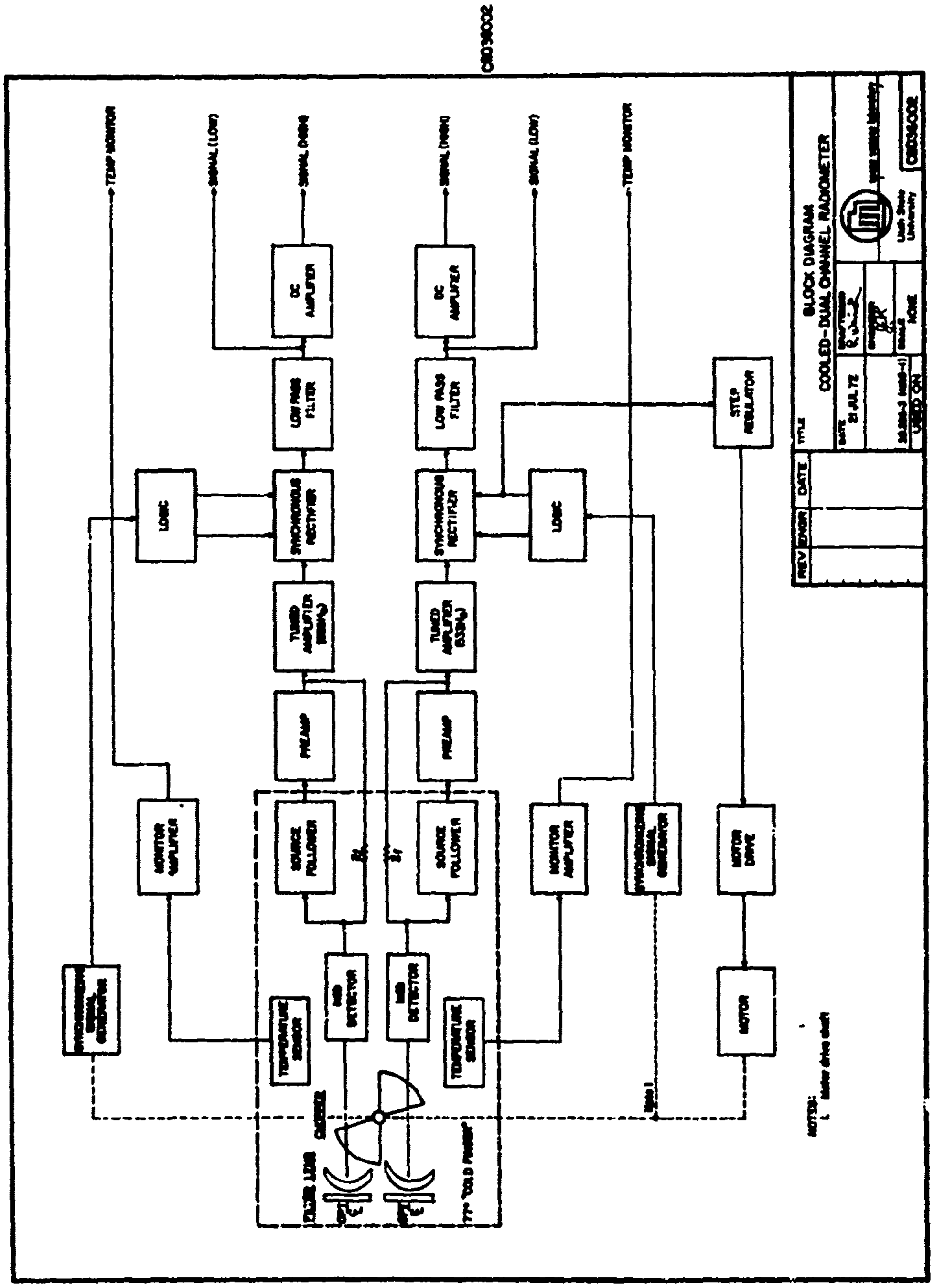

Figure 11. NR-3-1 block diagram.

vides the necessary impedance matching. To maximize the detectivity inherent in the cooled detector, a current mode feedback preamplifier with a ten megohm feedback resistor is used.

The preamplifier output is fed into a two stage, stagger-tuned amplifier. This amplifier is tuned to 533 Hz with with a 100 Hz bandwidth and a total gain of 40 db. The amplified signal is then fed into a synchronous rectifier where this signal is rectified to produce a dc output signal proportional to the radiation incident on the detector. By use of a synchronous rectifier noncoherent noise is minimized. A sync signal is generated by a photo diode which is illuminated through an aperture in the chopper drive shaft motor coupling. This signal is applied to the sync logic circuit where it is used to control the phase and symmetry of the synchronous rectifier. The rectifier output signal is then filtered in an active low pass filter which determines the overall system bandwidth from dc to an upper limit (f_2) ranging from 1 to 100 Hz depending on the requirements. The NR-3-1 system bandwidth was set at 5 Hz to obtain a high signal to noise ratio. The output from the filter is fed into a dc amplifier which is designed with a voltage gain of 20. Both high and low signal outputs are provided by connecting one output before the first amplifier and the other following it as shown in the block diagram.

The chopper motor speed is controlled by the step regulator which uses a slow motor detection circuit to increase the drive voltage whenever the motor speed falls below its proper value. This step is included so that the motor may operate at reduced voltage to conserve power as long as it runs at its proper speed. One of the synchronous rectifier drive signals serves as the motor speed indicator. When the motor is running at full speed (sync signal = 533 Hz) the motor is supplied with +20 volts. Whenever the sync pulse rate falls below 500 Hz, the full +28 volts are applied until the motor achieves full speed.

The temperature of the cold chamber is monitored using a forward biased silicon diode mounted inside the cold chamber adjacent to the detector. The forward voltage drop of the diode increases as the temp-

erature decreases, and this voltage is applied to the monitor amplifier. The output can be used to check operation of the cold chamber.

The system schematic diagrams are shown in Figures 12 and 13. For simplicity only one channel is shown, the second channel is identical. The combination of the InSb detector and electronics results in a system response that is extremely linear. Therefore, detailed computer data reduction may be accomplished by writing a linear responsivity function for each range. Calibration values are provided in Appendix A.

Circular Variable Filter Spectrometer, NS-1-1 (Astrobee D 30.205-4)

The circular variable filter spectrometer uses the same basic package and electronics as the dual-channel, cooled radiometer described in the previous section. The major difference is the circular variable filter which replaces the fixed filters and rotating chopper employed in the radiometer. The circular variable filter is constructed by applying an interference material to a 2½ in. diameter disk of substrate in such a manner that the thickness of the material varies linearly with angular displacement. The filter has a 4% resolution, i.e., the passband is 4% of the center wavelength. The filter used in the NS-1-1 system consisted of two 180° segments cemented together with opaque, zero transmittance reference masks attached at the two joints. The two-segment construction was necessary in order to cover the full 1.65 - 5.3 μ region. The filter is motor driven and allows the instrument to scan the desired spectral region once during each revolution. The masks provide a true zero reference signal for inflight calibration of the instrument. Figure 14 is a system block diagram for the NS-1-1 instrument.

Referring to the block diagram of Figure 14, incoming radiation is focused by a coated silicon lens on an indium antimonide detector after passing through the circular variable filter. The filter is motor driven at 2 rps and scans the 1.6 to 5.3 μ spectrum once each revolution. The signal from the detector is coupled to the preamp-

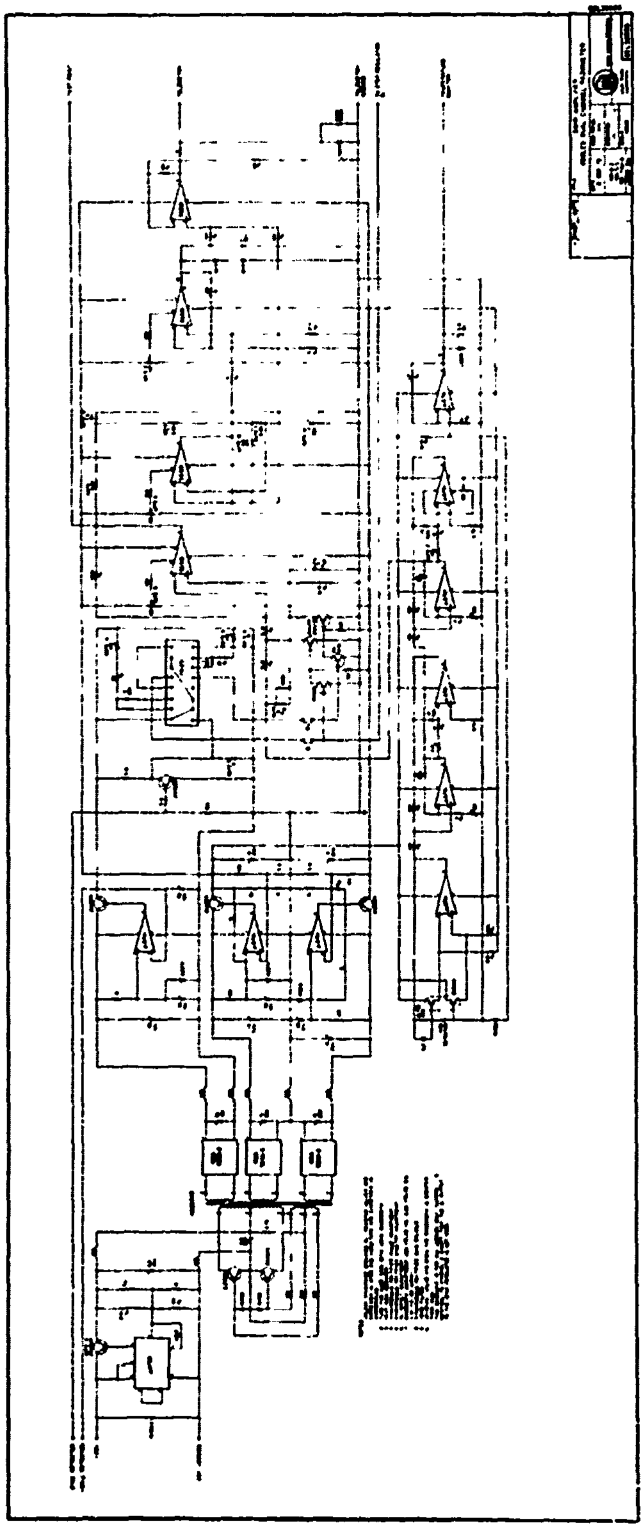

Figure 12. NR-3-1 amplifier schematic.

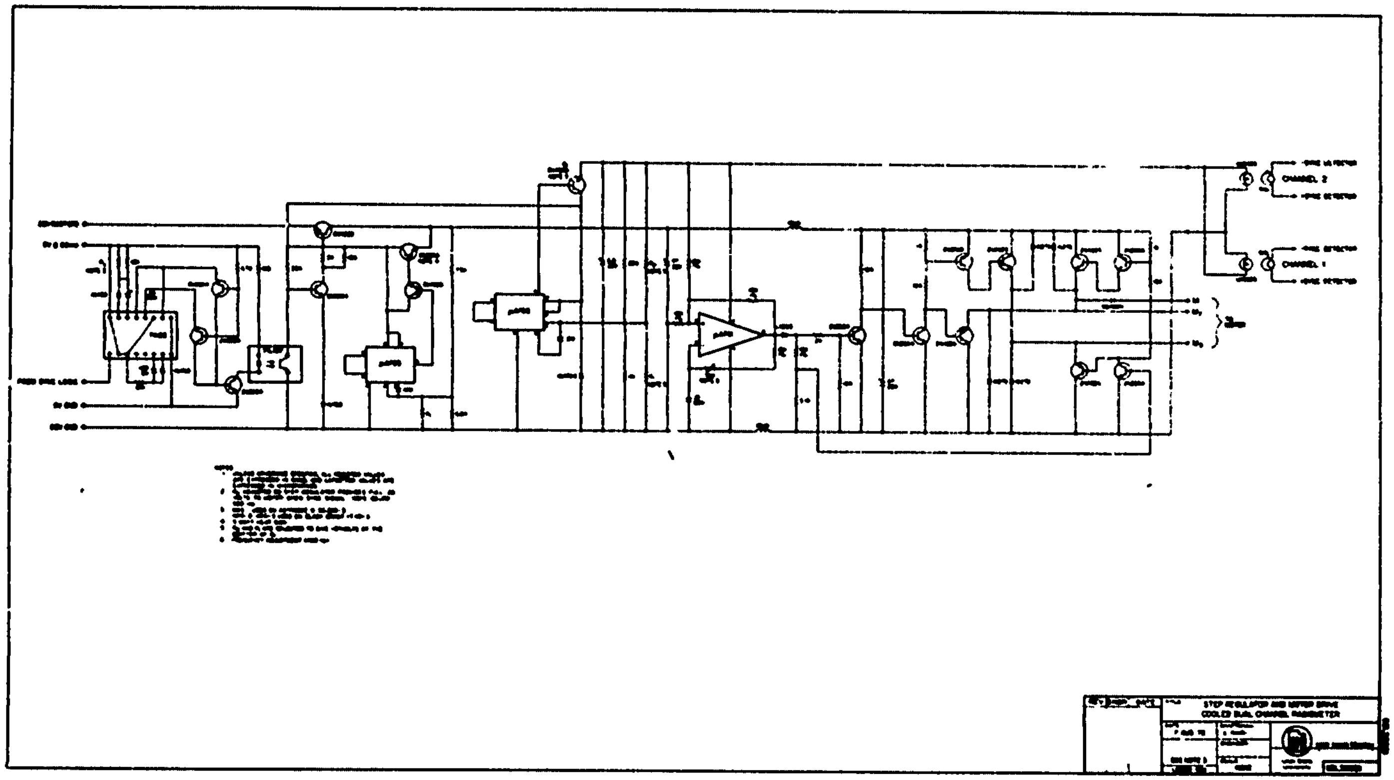

Figure 13. NR-3-1 step regulator and motor drive schematic.

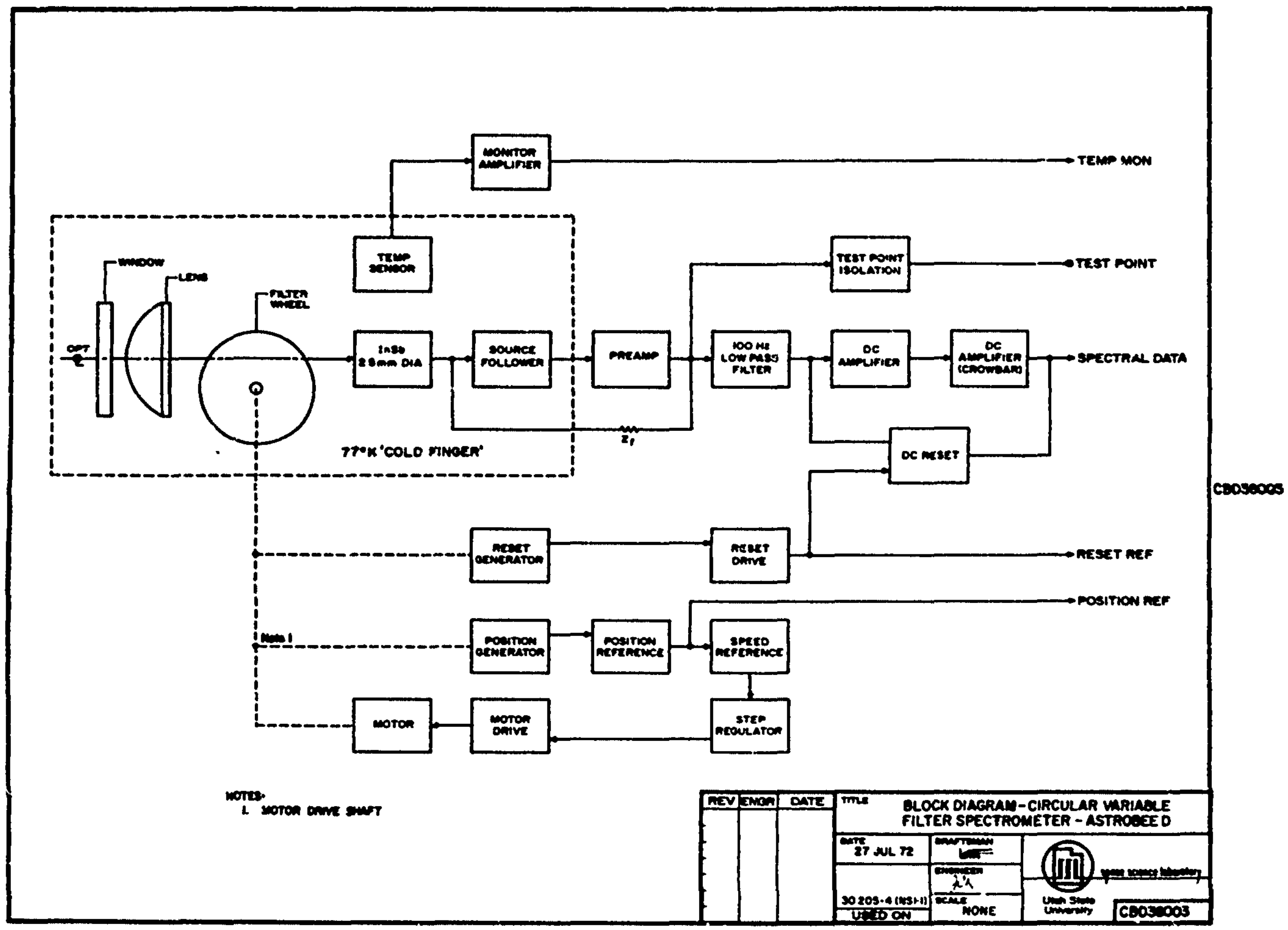

Figure 14. NS-1-1 block diagram.

lifier using a cooled source follower which provides the necessary impedance matching. To maximize the detectivity (D^*) inherent in the cooled detector, a current mode preamplifier with a ten megohm feedback resistor is used. The signal from the preamplifier is fed through an active low pass filter which determines the overall system bandwidth from dc to an upper limit (f_2) ranging from 1 to 100 Hz, depending on the requirements. The bandwidth for the NS-1-1 was set at 100 Hz to provide adequate resolving power using the circular variable filter. The CVF spectrometer is limited by the filter to a resolution of 4%.

After being filtered, the signal is amplified in a dc amplifier with a voltage gain of 50. The signal is then amplified in a variable gain dc amplifier. This amplifier is designed to have a voltage gain of 20 until the output reaches 2.5 volts after which the gain is unity providing a large dynamic range while maintaining good sensitivity to low signal levels.

Since DC amplifiers are often subject to drift problems a dc reset circuit has been included. This circuit receives its control signal from the reset generator via the reset drive. Once each cycle the large opaque mask on the circular variable filter is rotated in front of the detector yielding a zero output signal. This zero signal from the reset generator is fed into the reset drive where the pulse is shaped and an adjustable delay is provided to synchronize the reset pulse with the signal coming through the amplifier. The output from the reset drive is also telemetered to the ground where it is recorded and subsequently used to help determine filter position. Figure 15 shows the relationship of the reset reference signal to the filter position.

Also shown in Figure 15 is the position reference signal. The position generator consists of a series of apertures on the motor drive shaft which are illuminated by a small lamp. A series of pulses are generated as the aperture plate rotates, and these pulses are fed into the position reference circuit where they are shaped prior to telemetry. These pulses are also fed into the speed reference circuit where they are used to control the speed of the motor. If the motor speed is less than 1.8 rps, the step regulator furnishes a full 28 volts to the motor

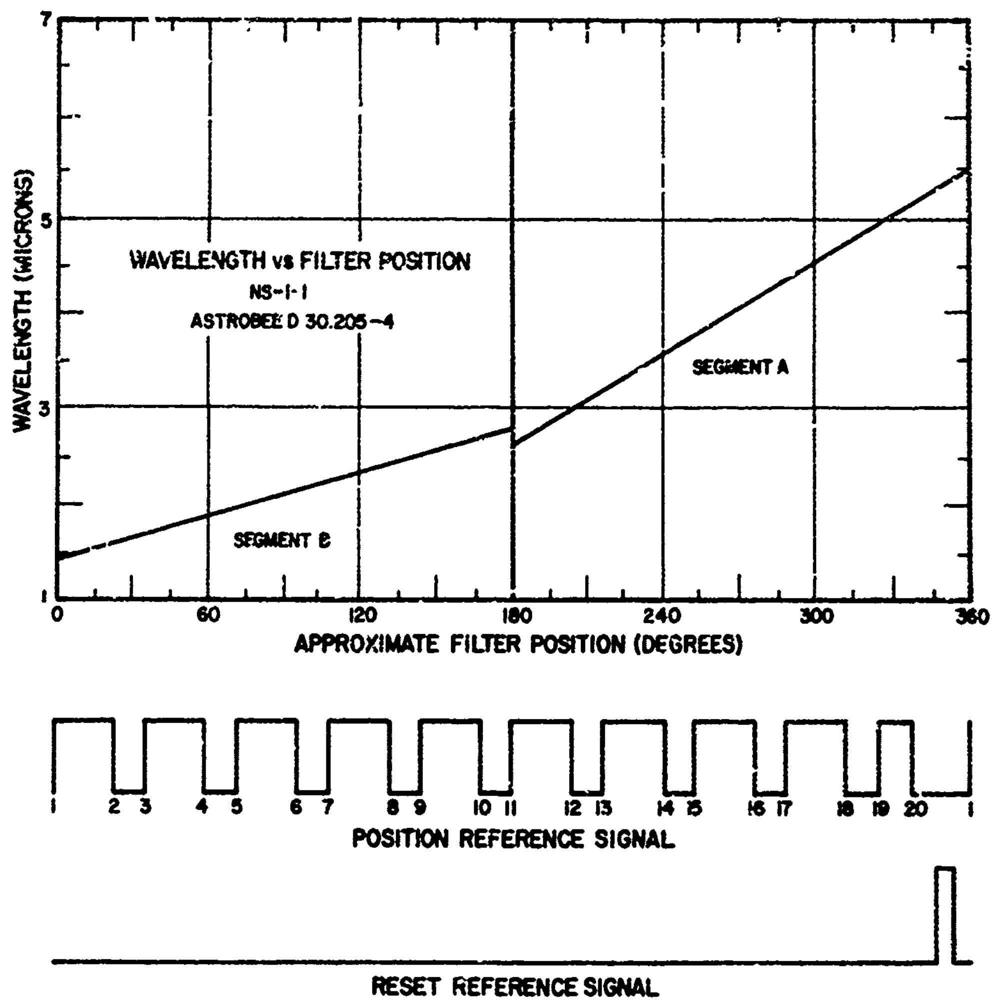

Figure 15. NS-1-1 filter position vs. reference signals. The reset reference signal and position reference signal are generated as the filter rotates providing a precise calibration of the center wavelength being passed by the filter. The approximate filter position in degrees has also been shown.

drive. After the motor has achieved its proper speed of 2 rps, the step regulator provides 20 volts to the motor drive to conserve power. Any time the speed of the motor drops below 1.8 rps, the full 28 volts are again applied to bring the motor back up to proper speed.

The temperature of the cold chamber is monitored using a forward biased silicon diode mounted inside the cold chamber adjacent to the detector. The forward voltage drop of the diode increases as the temperature decreases, and this voltage is applied to the monitor amplifier. The temperature monitor amplifier output can be used to check operation of the cold chamber.

Figure 16 is the system schematic diagram. The combination of the InSb detector and electronics results in a system response that is extremely linear. Therefore, detailed data computer reduction may be accomplished by writing a linear responsivity function for each dynamic range dominion (0 to 2.5 volts and 2.5 to 5.0 volts) in the same manner as for the radiometer. However, several additional steps must be taken. The center wavelength being sampled by the spectrometer must first be determined by referring to the reset reference pulse and position reference pulse as shown in Figure 15. The resolution element is then obtained for the center wavelength of interest by referring to Figure B-1, Appendix B. Finally, to determine the relationship of output volts to input radiance, refer to the responsivity curve, Figures B-2 to B-10, which most nearly represent the center wavelength. The same procedure must be followed for each wavelength of interest in the 1.6 to 5.3 μ spectrum.

Astrobee D 30.205-3 and Astrobee D 30.205-4 Support Instrumentation

Calibration Lamp

As noted previously in this report, since the optical and detecting portion of the two probe instruments were cooled, a cold cover was provided to keep the optics from frosting while in the dense lower atmosphere. To provide a check on the operation of the instruments, calibra-

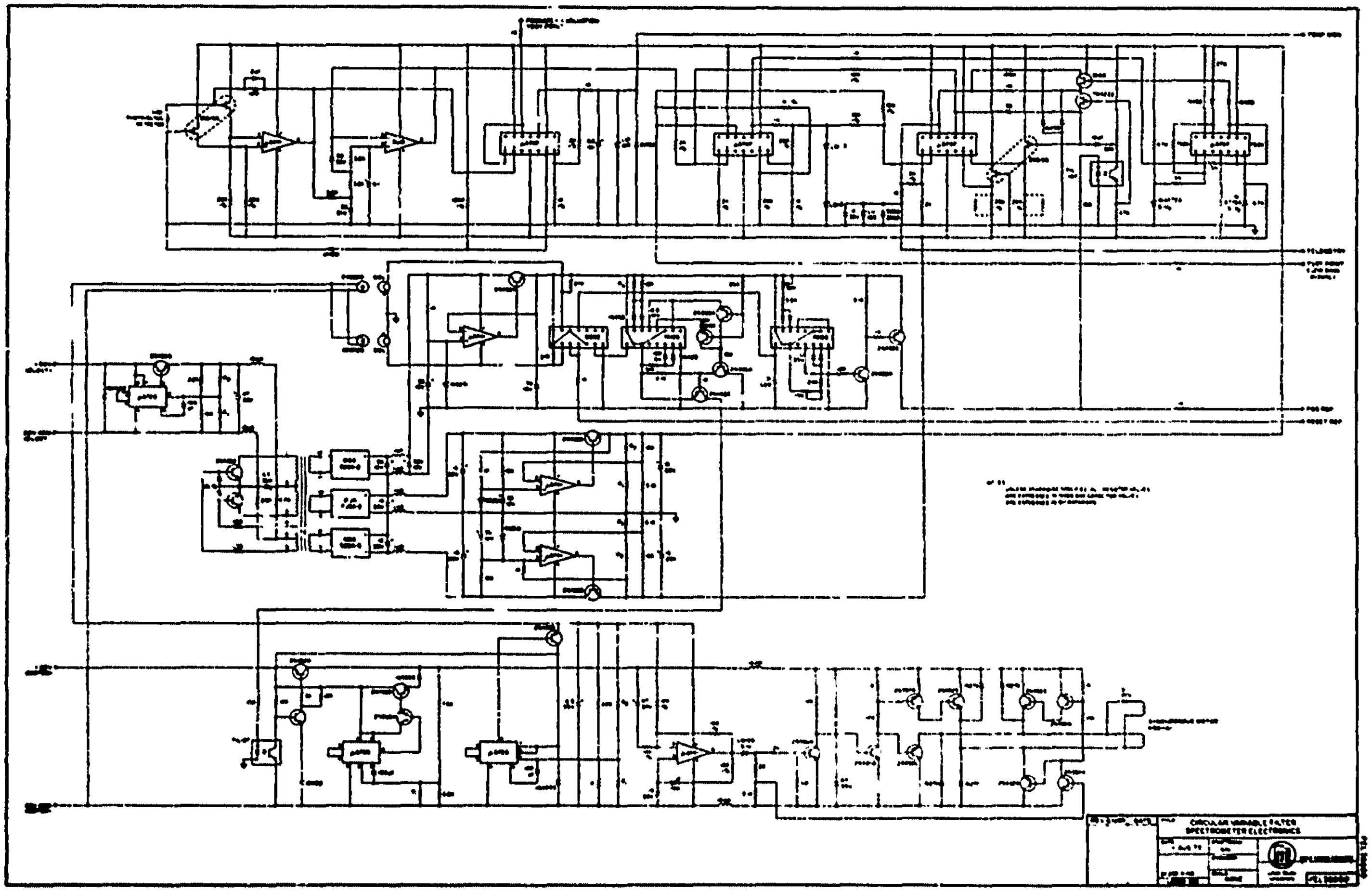

Figure 16. NS-1-1 schematic.

tion lamps were mounted into the cold covers above the detectors. These small lamps were driven by a circuit (Figure 6) which was included on the separation timer circuit board. The unit generated a pulse of 1 second duration with a repetition rate of 10 seconds. The calibration lamp circuit was activated when the arming pin was removed, thereby providing pulses to the instrument from early prelaunch time to the moment that the instrument cover was removed at about 50 km altitude.

Magnetometer

A Schonstedt magnetic aspect sensor, type RAM-5C, was used on each of the payloads. The sensor was mounted horizontally (at right angles to the major payload axis) near the center of the payloads. The positioning of the sensor is illustrated in Figure 17.

The magnetometer was included in the payload to provide an indication of payload orientation with respect to the earth's magnetic field

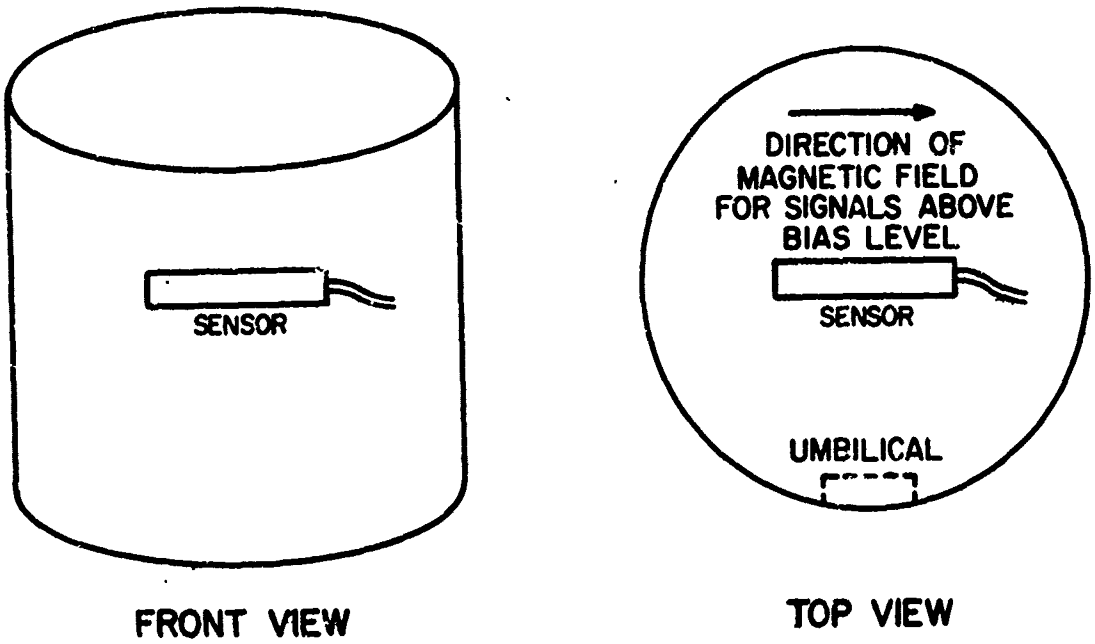

Figure 17. Magnetometer orientation.

and to determine the payload rotational velocity. A sample output waveform is shown in Figure 18 for a case of large coning. Each cycle represents one revolution of the rocket and so the frequency modulation represents the change in spin rate of the rocket. Since the maximum signal is obtained when the magnetic field is parallel to the sensor as shown in Figure 17, the amplitude modulation of the output signal indicates the degree of coning and the period represents the rate of precession. Magnetometer calibrations are included in the Appendices.

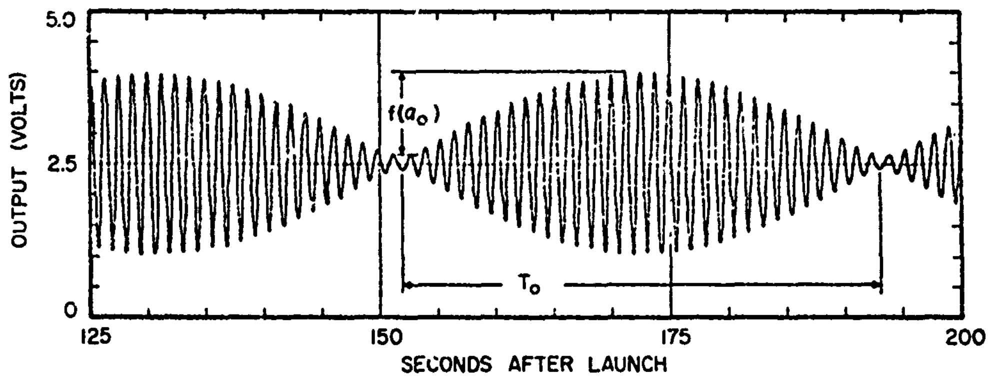

Figure 18. Sample magnetometer output for a case of large coning.

Baroswitch

A baroswitch was flown in each payload to provide a trajectory check point. Status of the baroswitch was monitored during the flight. Closure of the baroswitch occurred as shown in Table 3. With the baroswitch open, a zero volt output was obtained, and when the baroswitch was closed, the output changed to four volts. The failure of the baroswitch on the 30.205-4 payload to close as predicted is obviously a malfunction.

Temperature Monitors

In addition to the temperature monitor located in each instrument's optical compartment, three other temperature monitors were in-

TABLE 3

Baroswitch Closure for Astrobee D Payloads

Vehicle	Predicted Height	Measured Height*
A30-205-3	75,000 ft ± 3,000 ft	77,000 ft
A30-205-4	75,000 ft ± 3,000 ft	276,410 ft

*Determined from plot of height versus time of flight.

cluded in the Astrobee D payloads to determine the degree of heat transfer through the skin. The first sensor was attached in a depression approximately .025" deep on the inside of the payload skin just aft of the primary instrument. The second sensor was placed near the first, on the inside surface of the payload skin. The third sensor was placed in the center of the electronics package. By monitoring the outputs from the first two sensors, the rate of skin heating can be determined, and by monitoring the third sensor output, the rate at which heat is transferred to the electronics can be determined.

Initial testing of the Astrobee D rocket by Space General indicated that nosetip skin temperatures approached 400°F during the first portion of the flight [*Jenkins, et al.*, 1970]. Knowledge of the rate of heat transfer to the inside of the payload is important to assess the possible danger to electronics components and because in the case of cooled measuring devices, warming of the instrument could lead to erroneous data. Temperature data received from the Astrobee D 30.205-3 and 30.205-4 payloads indicated that skin temperatures approached 400°F. The electronics compartment temperature remained cool, however, and only increased about 5°F during the flight. The temperature monitor calibration is included in Appendix A.

Telemetry

The Astrobee D payloads utilized a FM transmitter with four subcarriers. The transmitter carrier frequency was 243.6 MHz. Outputs

from the supporting instruments and some of the prime instruments' outputs were commutated in a sixteen segment, sixteen frames-per-second electronic commutator. Figures 19 and 20 are block diagrams of the telemetry systems for the Astrobee D 30.205-3 and 30.205-4 payloads. Shown in the block diagrams are the various subcarrier assignments. Figure 21 is a schematic diagram of the sixteen segment commutator. Segment assignments are found in the Appendices.

All telemetry systems with the exception of the 16 segment commutator were supplied by AFCRL (LCS) for installation in the payload by USU personnel. Responsibility for the telemetry system including ground equipment remained with AFCRL. The subcarriers and mixer amplifiers were Vector micro-miniature Series 11, mounted in a Vector MMM-622 micro-miniature mount. Subcarrier assignments are also found in the Appendices. The telemetry transmitter was a Vector model TR1125 FM transmitter with a five-watt output. The output from the transmitter was fed into an antenna consisting of four $\frac{1}{8}''$ x 12 $\frac{1}{2}''$ stainless steel rods set at 90° intervals around the skin and protruding at an angle of 45°. These antennas are shown in Figure 9. The phasing harness was connected to give a right-circularly polarized pattern as viewed from the front of the rocket.

RESULTS

The Astrobee D payloads were highly successful in that all systems functioned properly and good data were received. The nosetip separation demonstrated a new technique by separating from the rear and removing the primary instrument cold covers. In both cases nosetip ejection was successful and little coning action was imparted to the payload during the separation sequence. The Astrobee D 30.205-3 and 30.205-4 trajectories are shown graphically in Figure 22. Trajectory listings are found in Appendix C.

The successful operation of the Astrobee D payloads demonstrated the practicality of using small rockets for making auroral measurements. These smaller payloads can give investigators an increased degree of measurements flexibility through reduced cost and ease of han-

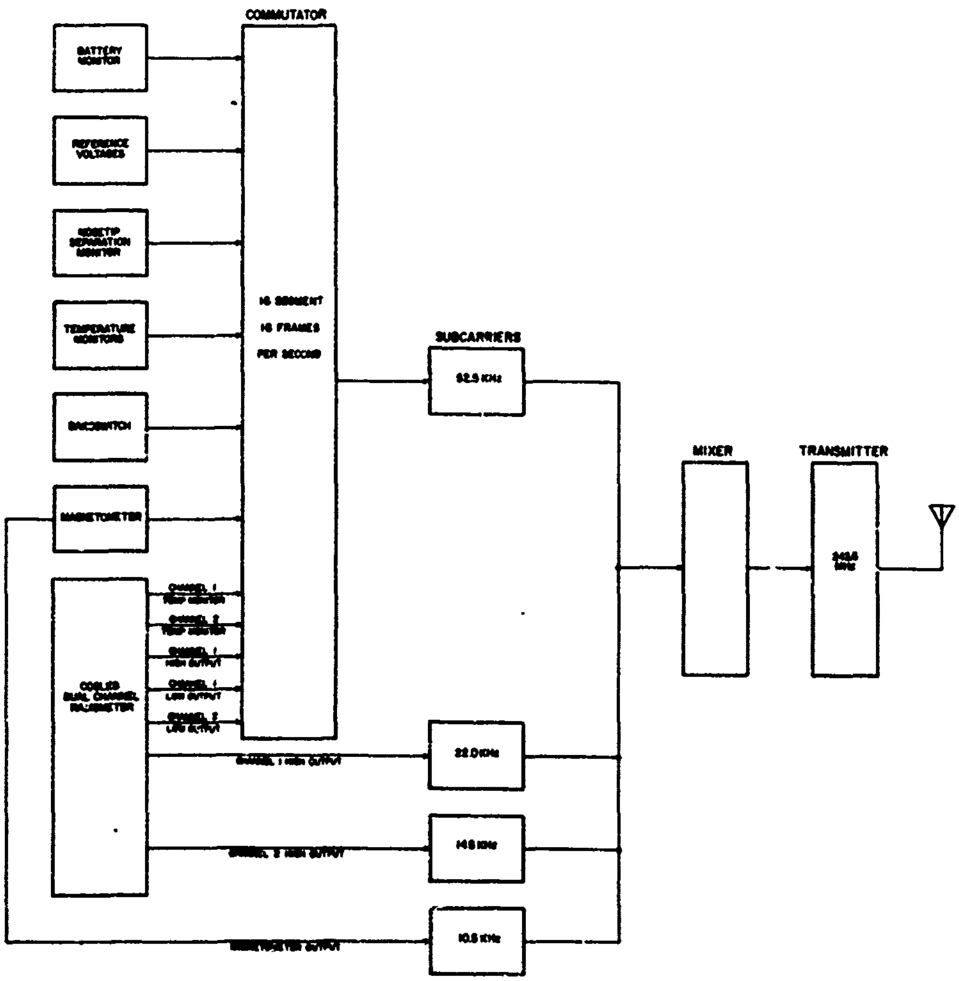

Figure 19. Astrobee D 30.205-3 telemetry block diagram.

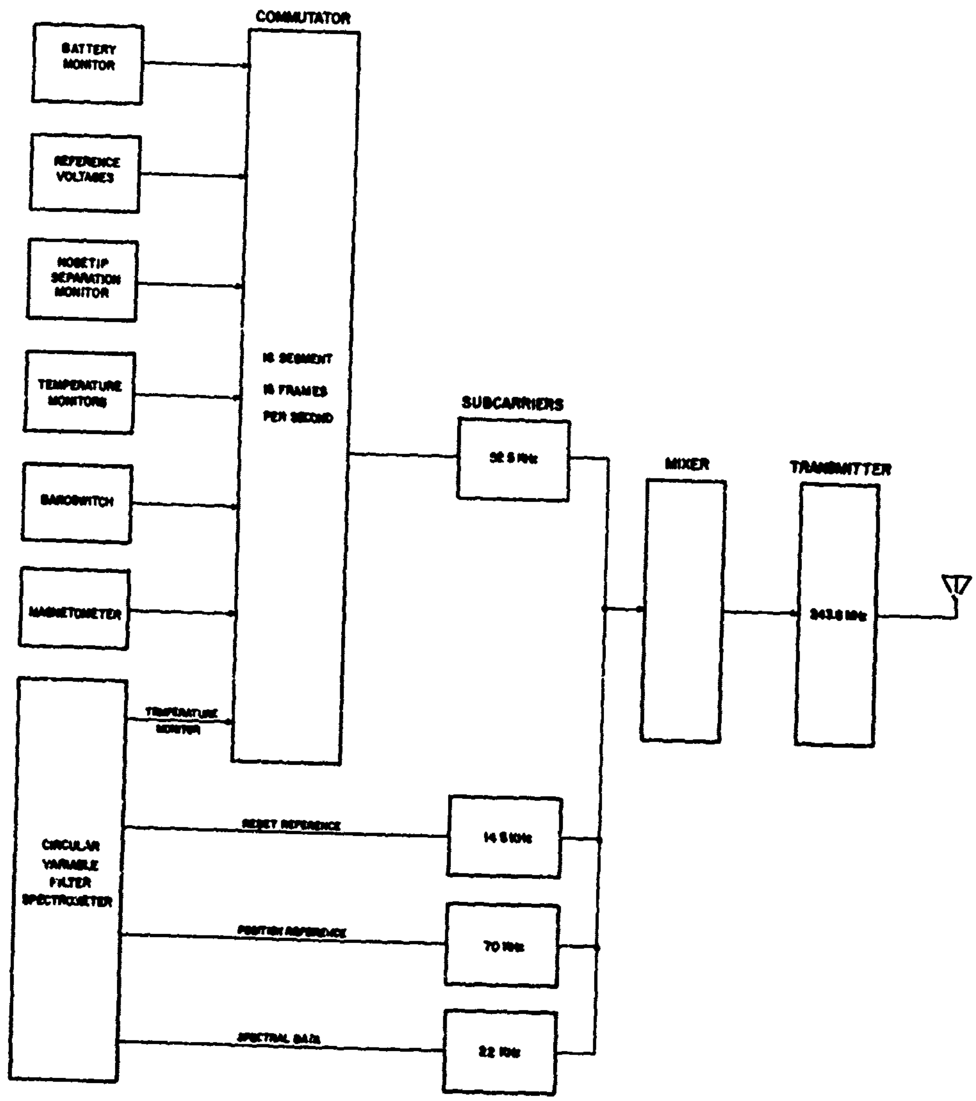

Figure 20. Astrobee D 30.205-4 telemetry block diagram.

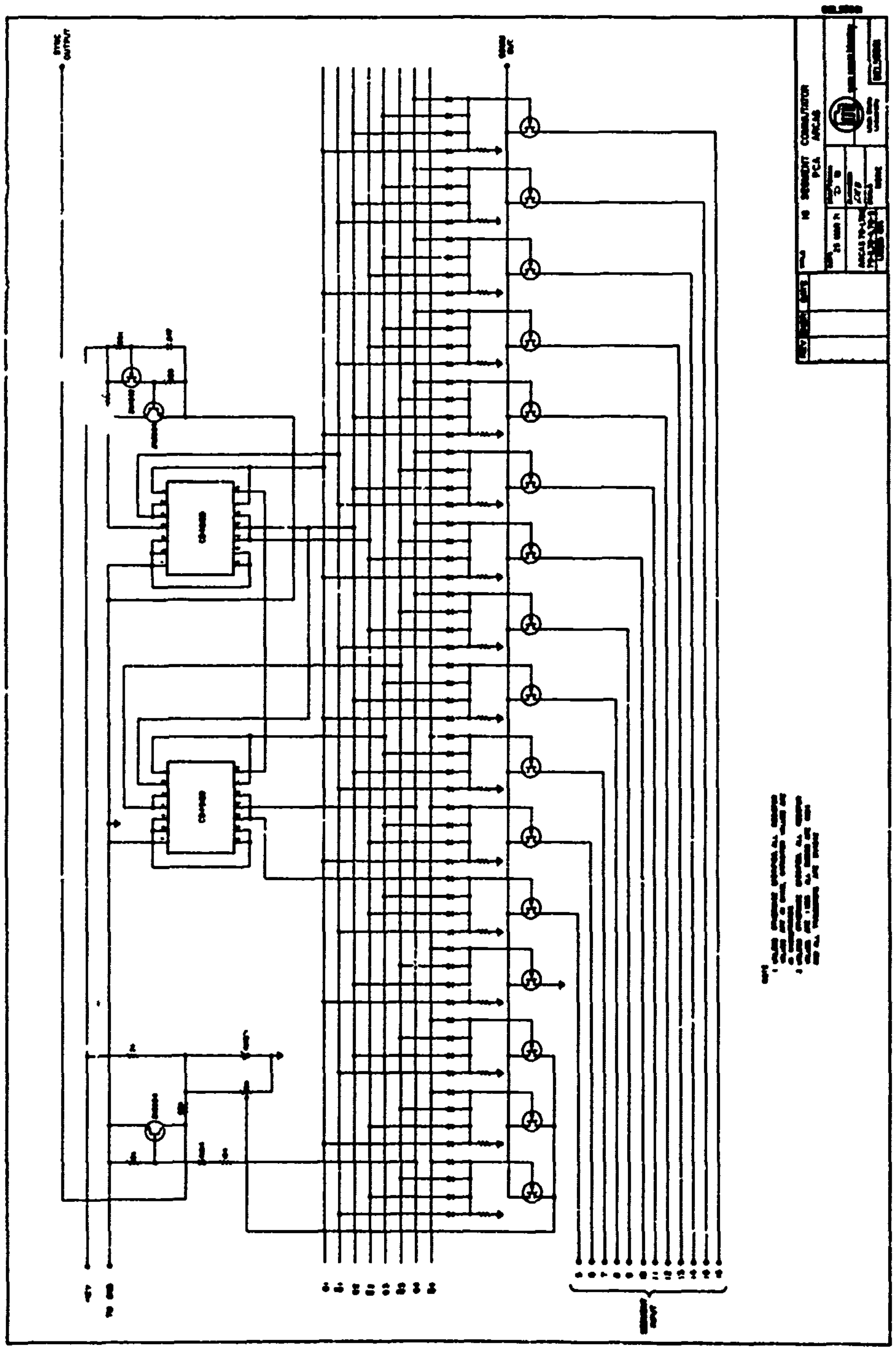

Figure 21. Sixteen segment commutator schematic.

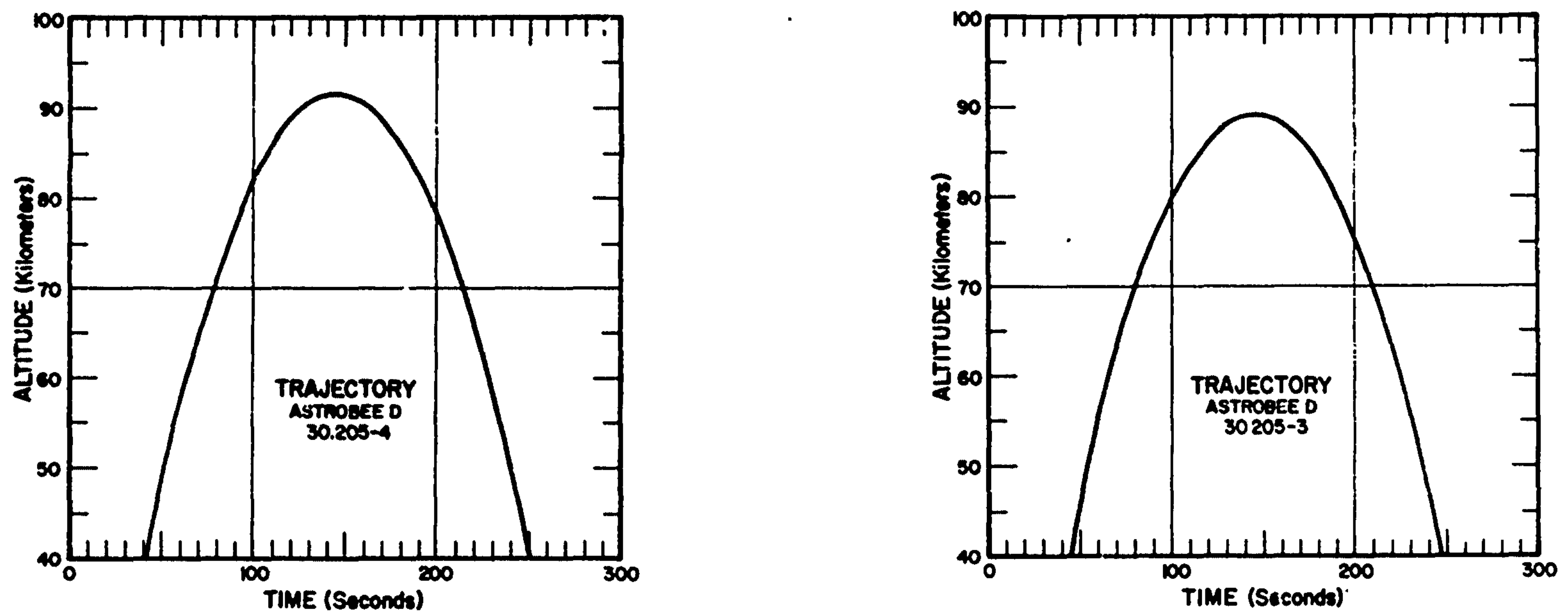

Figure 22. Astrobee D 30.205-3 and Astrobee D 30.205-4 trajectories.

dling. By using several such payloads, it would be possible to make measurements simultaneously at several locations or to obtain a chronological record of a particular event by sequentially firing several rockets from the same location.

The two new instruments fulfilled the design objectives of developing new instruments for auroral research for use on small rockets. The use of cooled optics and sensors on the primary instruments permitted measurements in the infrared region without contamination from the instrument itself. Preliminary analysis indicates that both the cooled, dual-channel radiometer and the cooled, circular variable filter spectrometer provided good data and functioned as planned. The radiometer data provided insight into the intensity of the short wave infrared radiation bands and increased our knowledge of the OH processes. Good spectral data were received from the spectrometer which furthered our understanding of the short wave infrared spectrum. Complete processing of the data is in progress and the results of these flights will be the subject of future reports.

Perhaps the most significant of the results from the Astrobee D flights has been the advancement of ionospheric measurements technology. The engineering principles used on the Astrobee D 30.205-3 and 30.205-4 payloads are being refined and are of great value in designing the current set of rockets under a subsequent contract. Through knowing the intensity of the short wave infrared radiation, improvements in the instruments have been made which will allow more efficient measurements. Substantial weight reductions in the new radiometers and spectrometers have resulted in a more comprehensive Astrobee D instrumentation package which will lead to even better results from future flights.

REFERENCES

Baker, K. D. and G. D. Allred, Arcas rocket instrumentation development for mesospheric measurements, *USU Scientific Report No. 1, AFCRL 72-0472*, Contract F19628-70-C-0302, Space Science Laboratory, Utah State University, Logan, June 1972.

Burt, D. A., L. C. Howlett, and R. J. Bell, Small rocket instrumentation for Polar Cap Absorption measurements, *USU Scientific Report No. 2, AFCRL 72-0460,* Contract F19628-70-C-0302, Space Science Laboratory, Utah State University, Logan, July 1972.

Burt, D. A., J. C. Kemp, L. C. Howlett, E. F. Pound, G. K. LeBaron, and G. D. Allred, ICECAP 72 -- A rocket measurements program for the investigation of auroral infrared emissions -- Black Brant 17.110-3, *USU Scientific Report No. 4, AFCRL - ,* Contract F19628-70-C-0302, Space Science Laboratory, Utah State University, Logan, 1972.

Jenkins, R. B., J. P. Taylor, T. B. Browne, L. A. Biggs, Astrobee D -- An advanced technology meteorological rocket vehicle, *AIAA Paper No. 70-1387,* New York, December 1970.

Megill, L. R., A. M. Despain, D. J. Baker, and K. D. Baker, Oxygen atmospheric and infrared atmospheric bands in the aurora, *J. Geophys. Res., 75,* 4775, 1970.

Noxon, J. F., Auroral emission from $O_2(^1\Delta_g)$, *J. Geophys. Res., 75,* 1879, 1970.

Stair, A. T. Jr., E. R. Huppi, B. P. Sandford, R. E. Murphy, R. R. O'Neil, and A. M. Hart, Infrared investigations of aurora and airglow, *The Radiating Atmosphere,* edited by B. M. McCormac, D. Reidel Publishing Co., Dondrecht, Holland, 1971.

Zipf, E. C., W. L. Bonst, and T. M. Donahue, A mass spectrometer observation of NO in an auroral arc, *J. Geophys. Res., 75,* 6371, 1970.

APPENDIX A

NR-3-1

CALIBRATION

A-1a

TABLE A-1

Commutator Segment Assignments -- Astrobee D 30.205-3

Segment No.	Assignment	Segment No.	Assignment
1	+5 volt reference	9	Skin temp. mon. No. 2
2	+5 volt reference	10	Magnetometer bias
3	+5 volt reference	11	Channel 2 low output
4	0 volt reference	12	Baroswitch output
5	Channel 1 high output	13	Nosetip separation switch out.
6	Electronics temp. mon.	14	Channel 1 Det. Temp. Mon.
7	Channel 1 low output	15	Channel 2 Det. Temp. Mon.
8	Skin temp. mon. No. 1	16	Battery voltage mon. (+28 v)

Note: Commutator frame rate = 16 frames per second.

TABLE A-2

Subcarrier Oscillator Assignments -- Astrobee D 30.205-3

Assignment	Frequency (kHz)
Channel 1 high output	22.0
Channel 2 high output	14.5
Commutator	52.5
Magnetometer	10.5

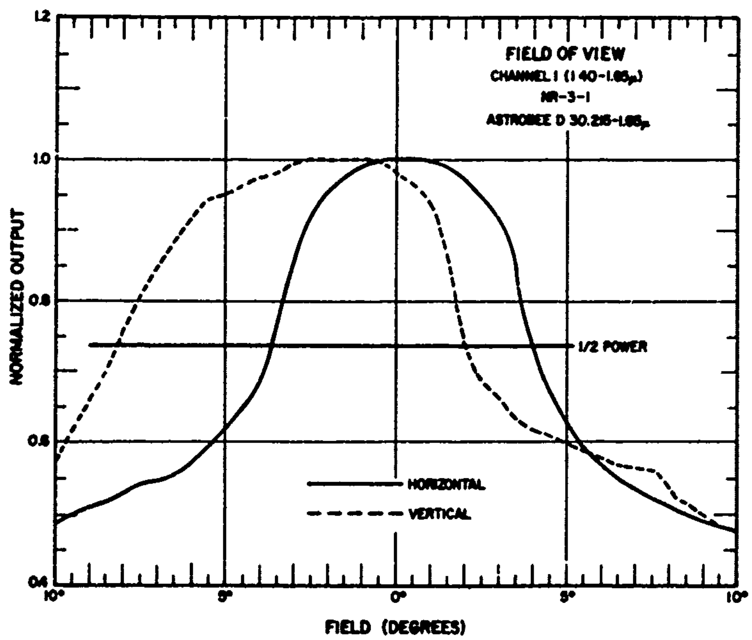

Figure A-1. Field of view---channel 1, NR-3-1.

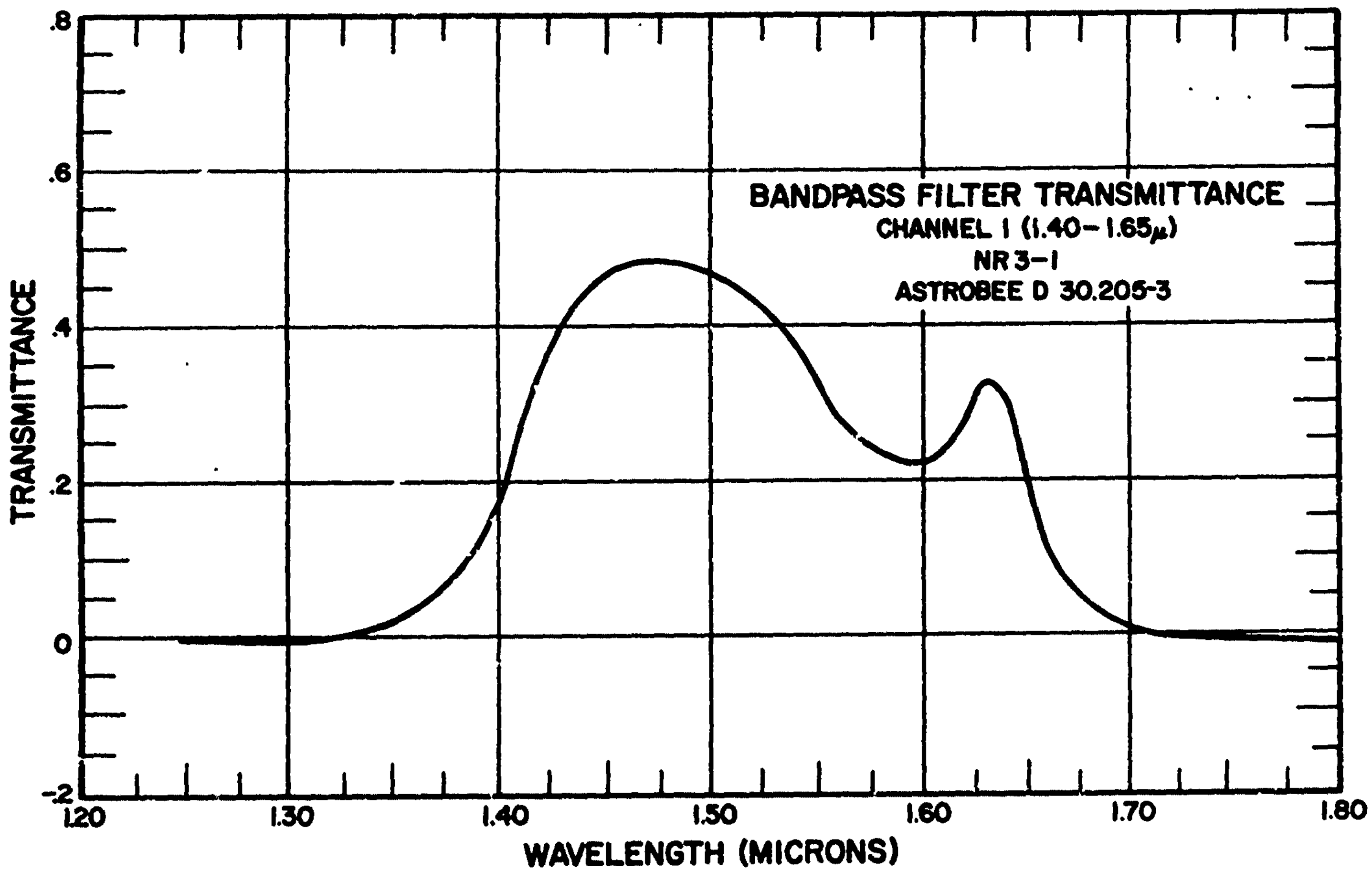

Figure A-2. Bandpass filter transmittance---channel 1, NR-3-1.

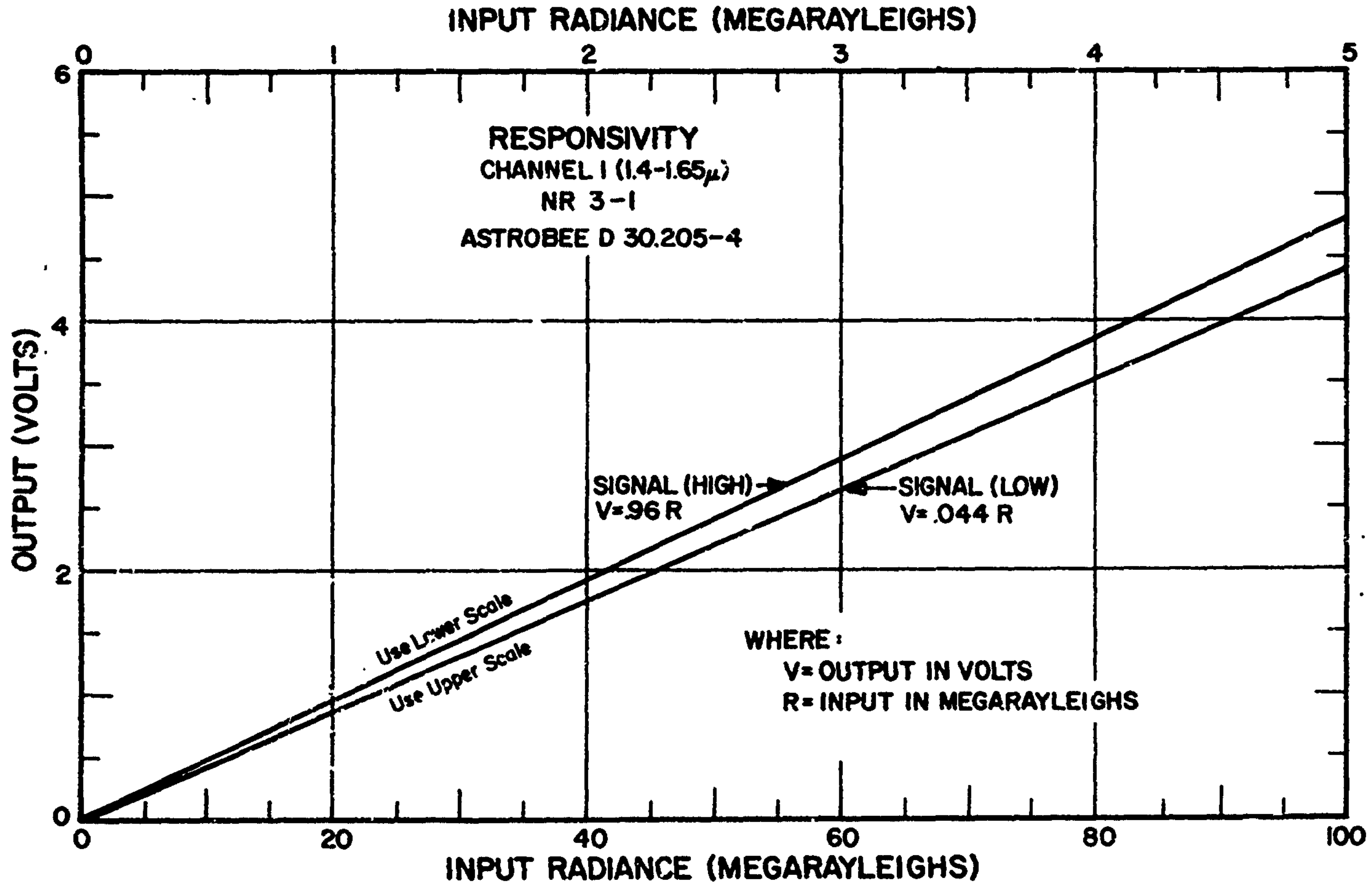

Figure A-3. Responsivity---channel 1, NR-3-1.

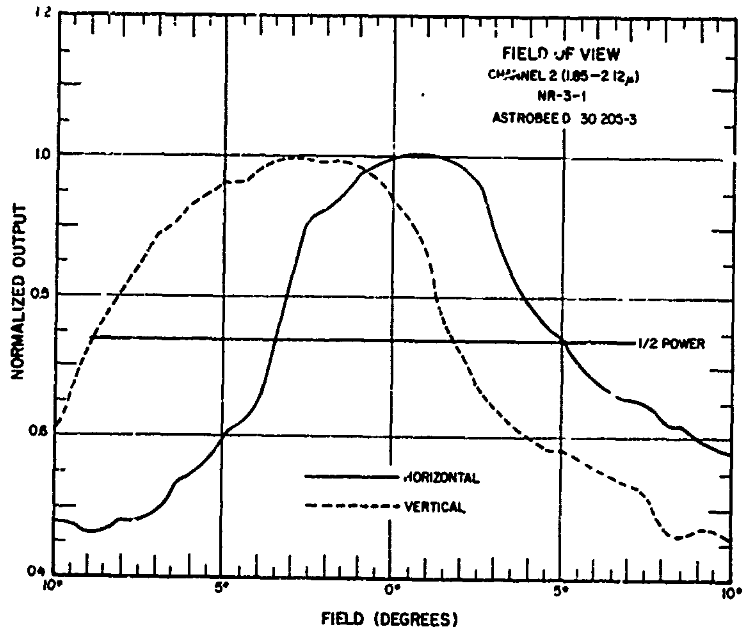

Figure A-4. Field of View---channel 2, NR-3-1.

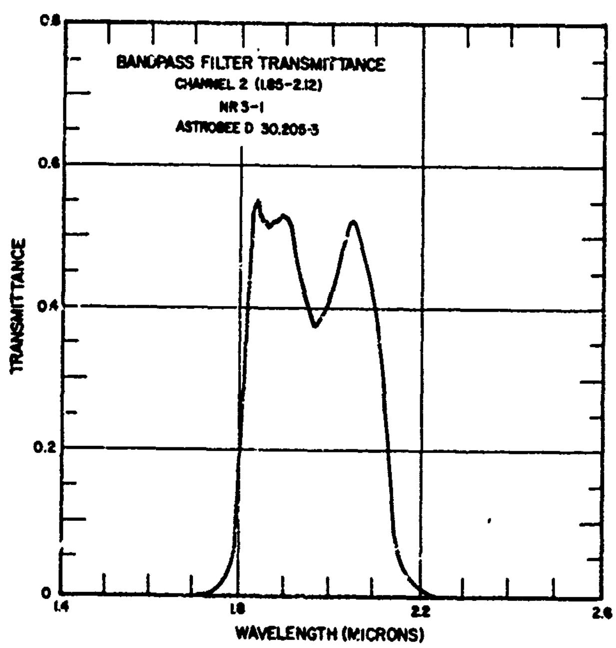

Figure A-5. Bandpass filter transmittance---channel 2, NR-3-1.

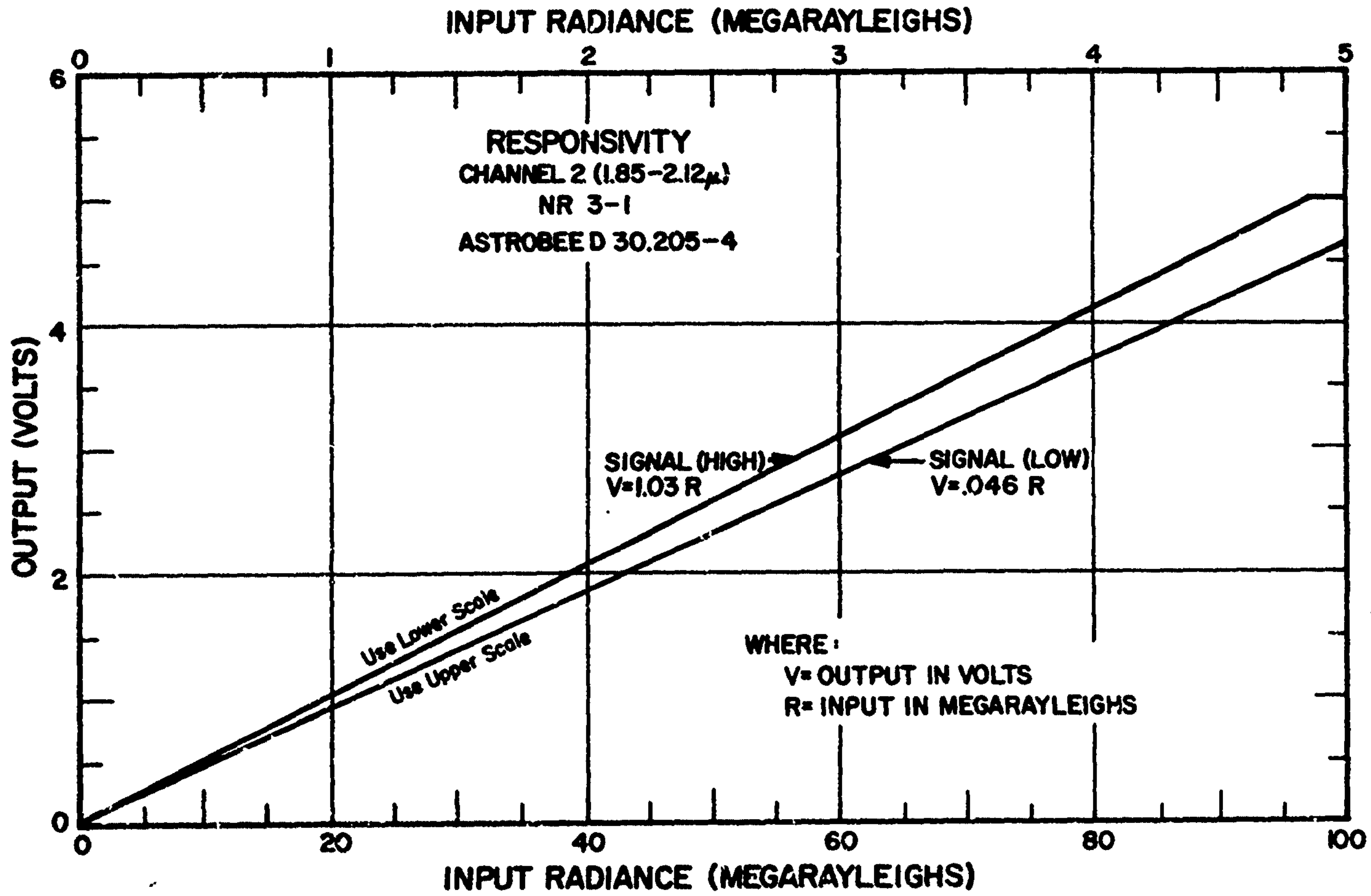

Figure A-6. Responsivity---channel 2, NR-3-1.

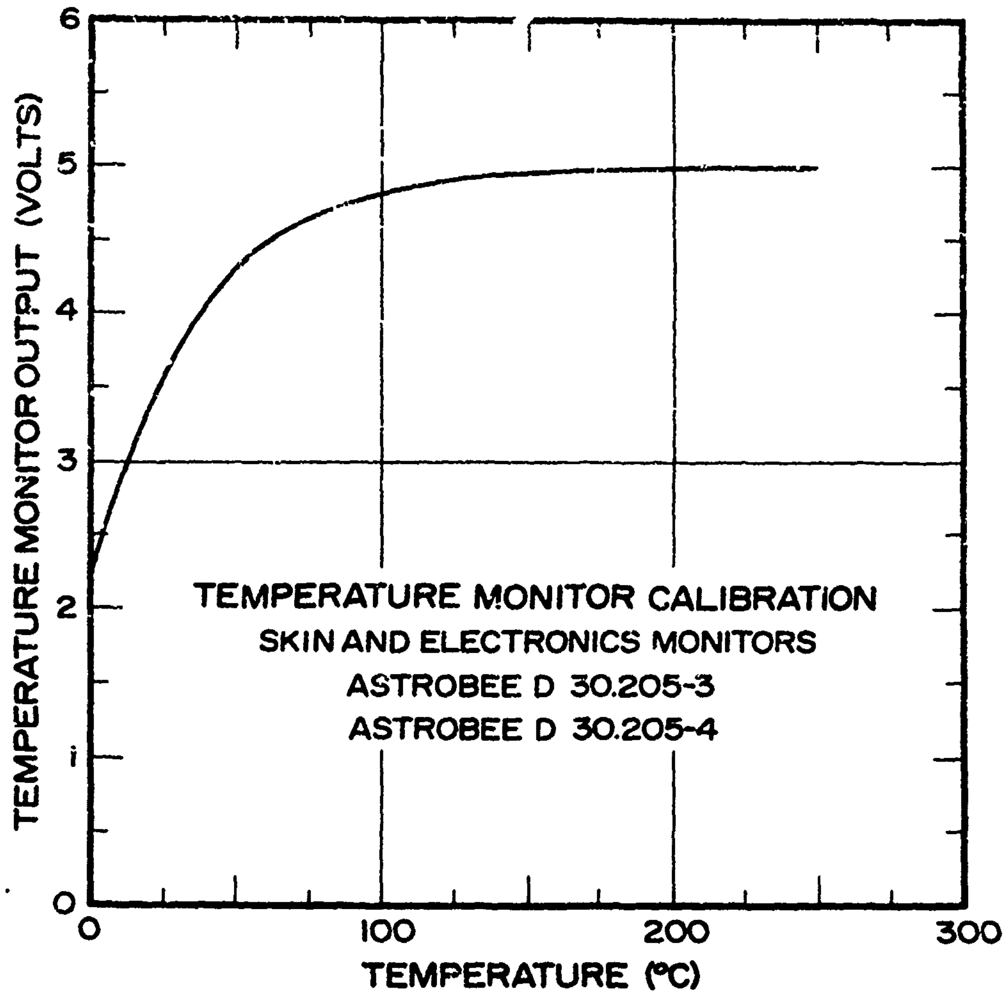

Figure A-7. Temperature monitor calibration---skin and electronics monitors.

APPENDIX B

NS-1-1

CALIBRATION

B-1a

TABLE B-1

Commutator Segment Assignments -- Astrobee D 30.205-4

Segment No.	Assignment	Segment No.	Assignment
1	+5 volt reference	9	Skin temp. mon. No. 2
2	+5 volt reference	10	Magnetometer bias
3	+5 volt reference	11	Detector temp. mon.
4	0 volt reference	12	Baroswitch output
5	Magnetometer output	13	Nosetip separation switch out
6	Electronics temp. mon.	14	Magnetometer output
7	Detector temp. mon.	15	Not used
8	Skin temp. mon. No. 1	16	Battery voltage mon. (+28 v)

Note: Commutator frame rate = 16 frames per second.

TABLE B-2

Subcarrier Oscillator Assignments -- Astrobee D 30.205-4

Assignment	Frequency (kHz)
Spectral data	22.0
Reset reference	14.5
Position reference	70.0
Commutator	52.5

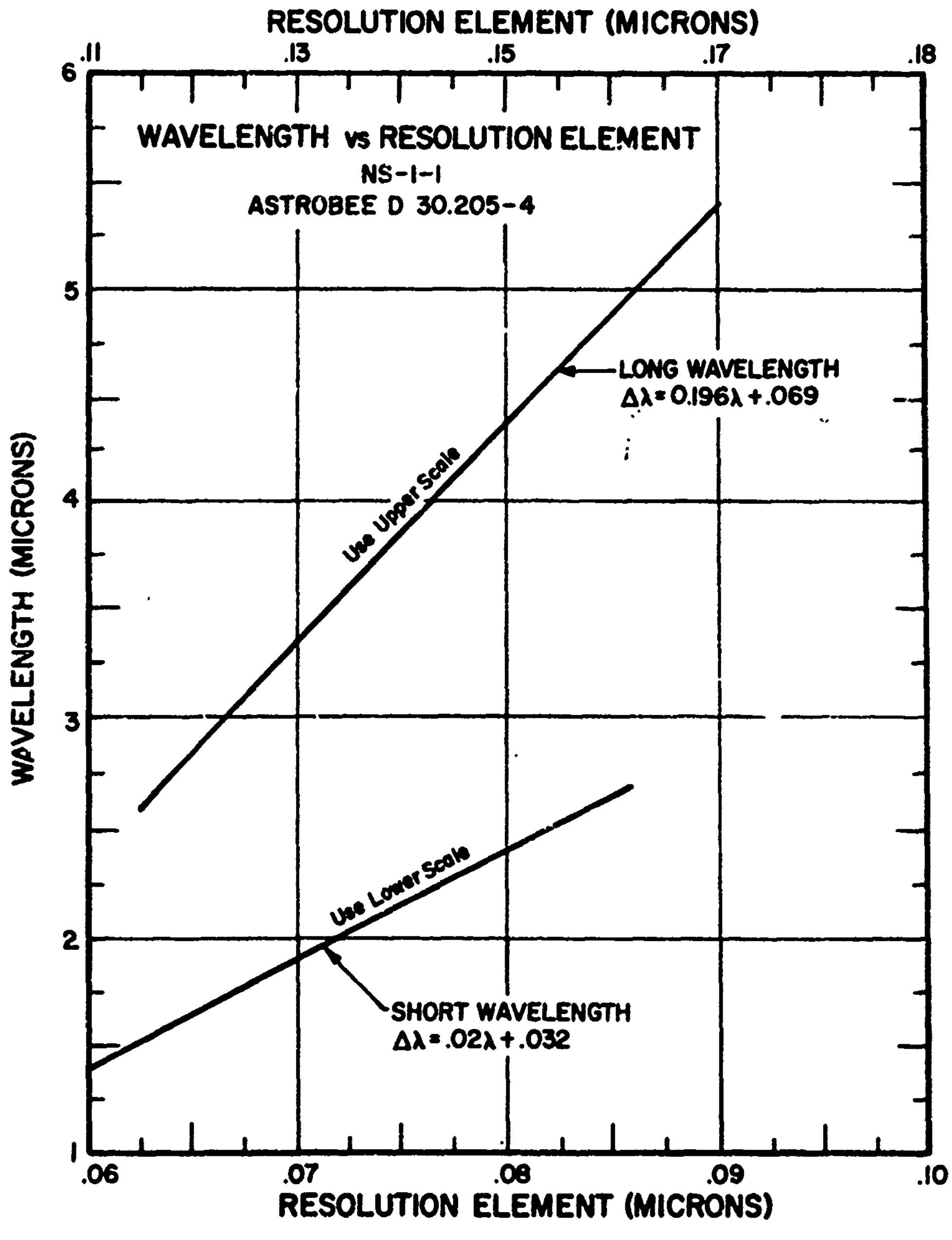

Figure B-1. Wavelength vs resolution element---NS-1-1.

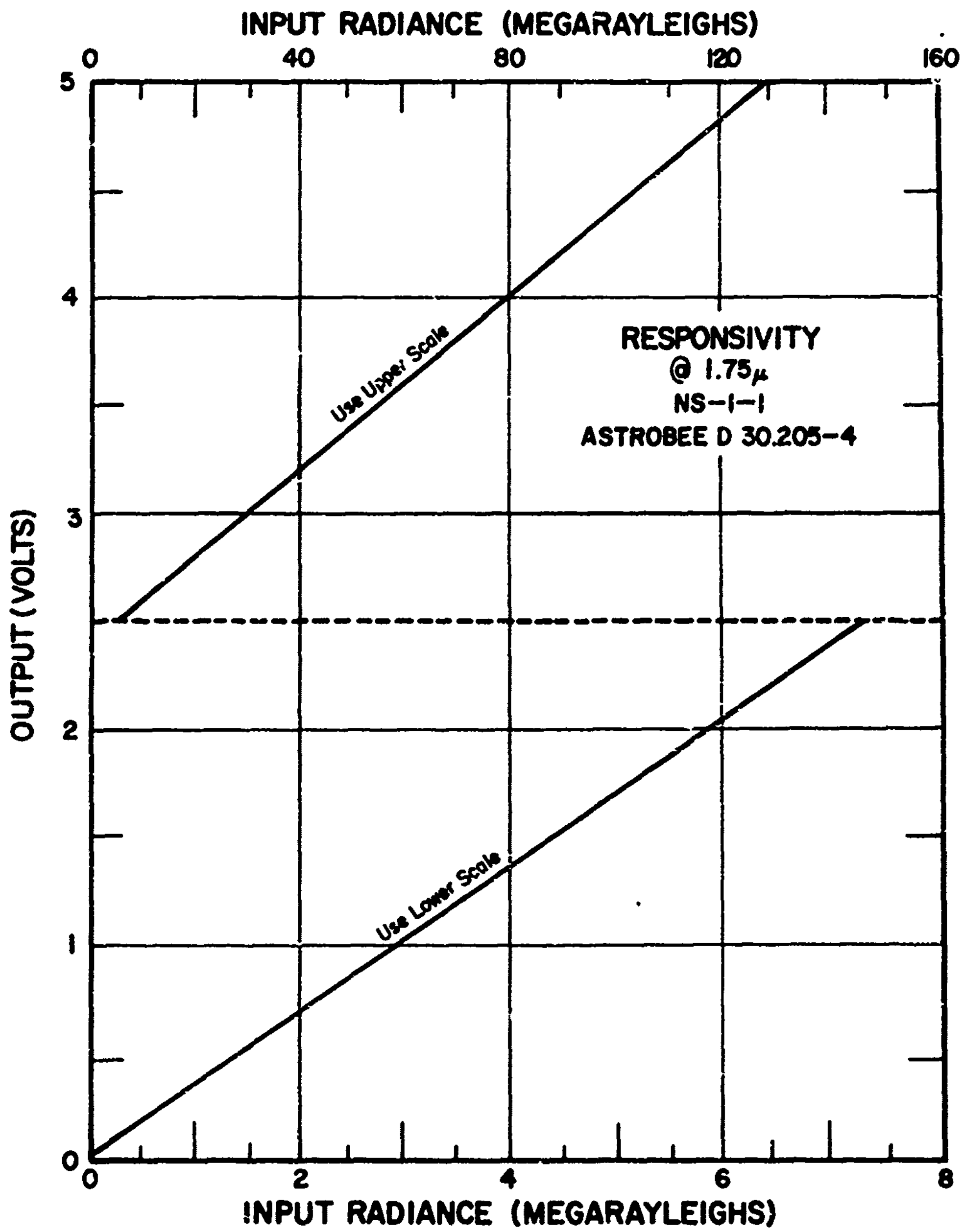

Figure B-2. Responsivity @].75μ---NS-1-1.

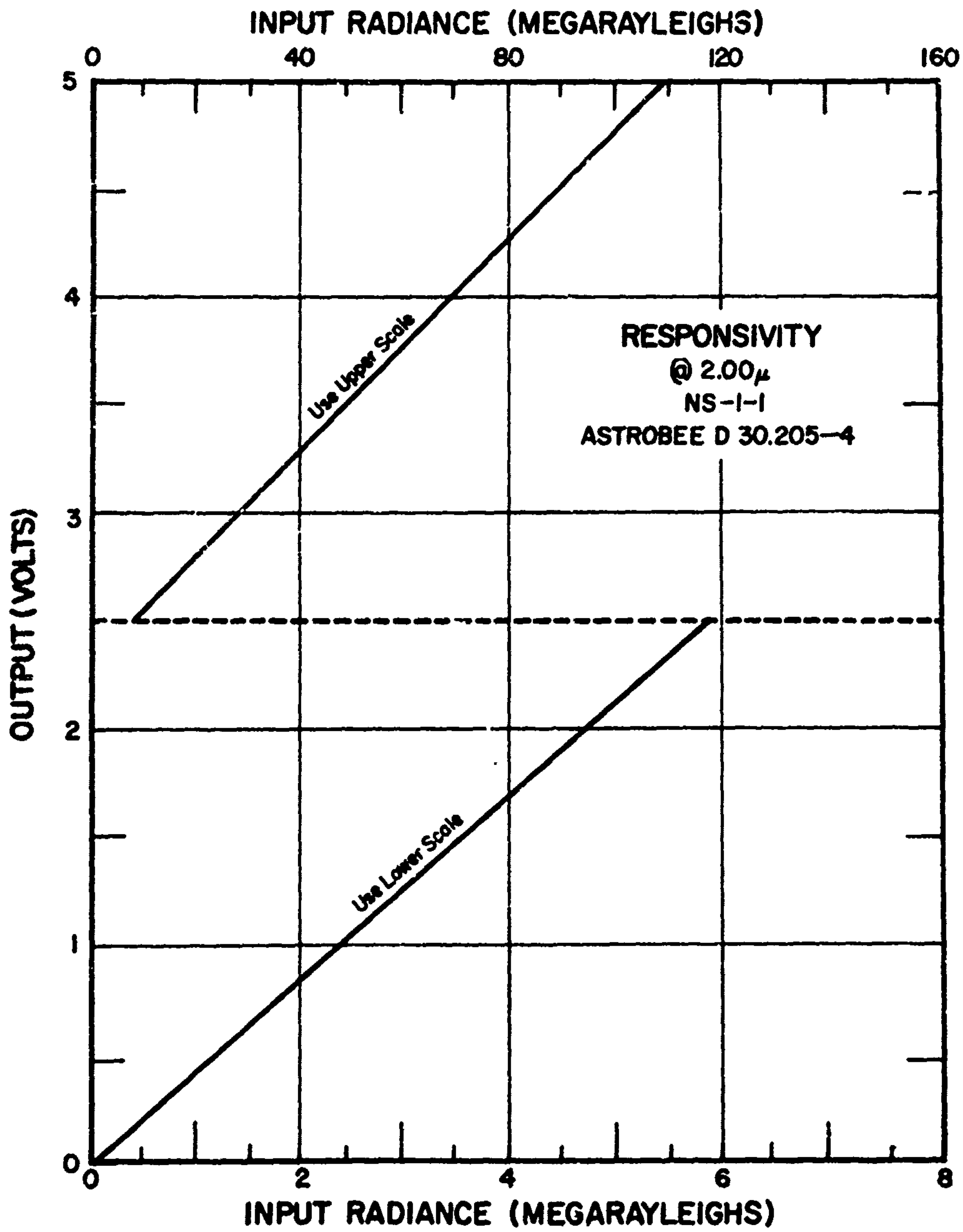

Figure B-3. Responsivity @ 2.00μ---NS-1-1.

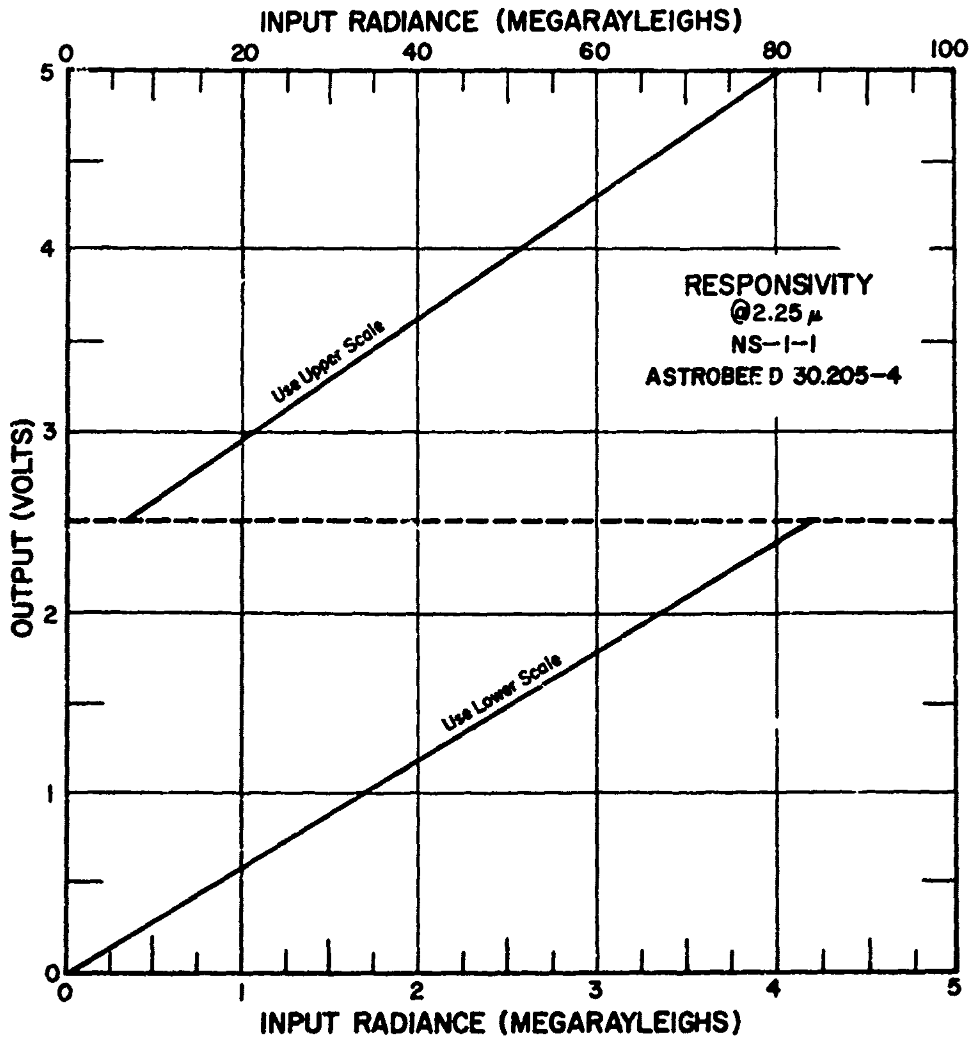

Figure B-4. Responsivity @ 2.25μ---NS-1-1.

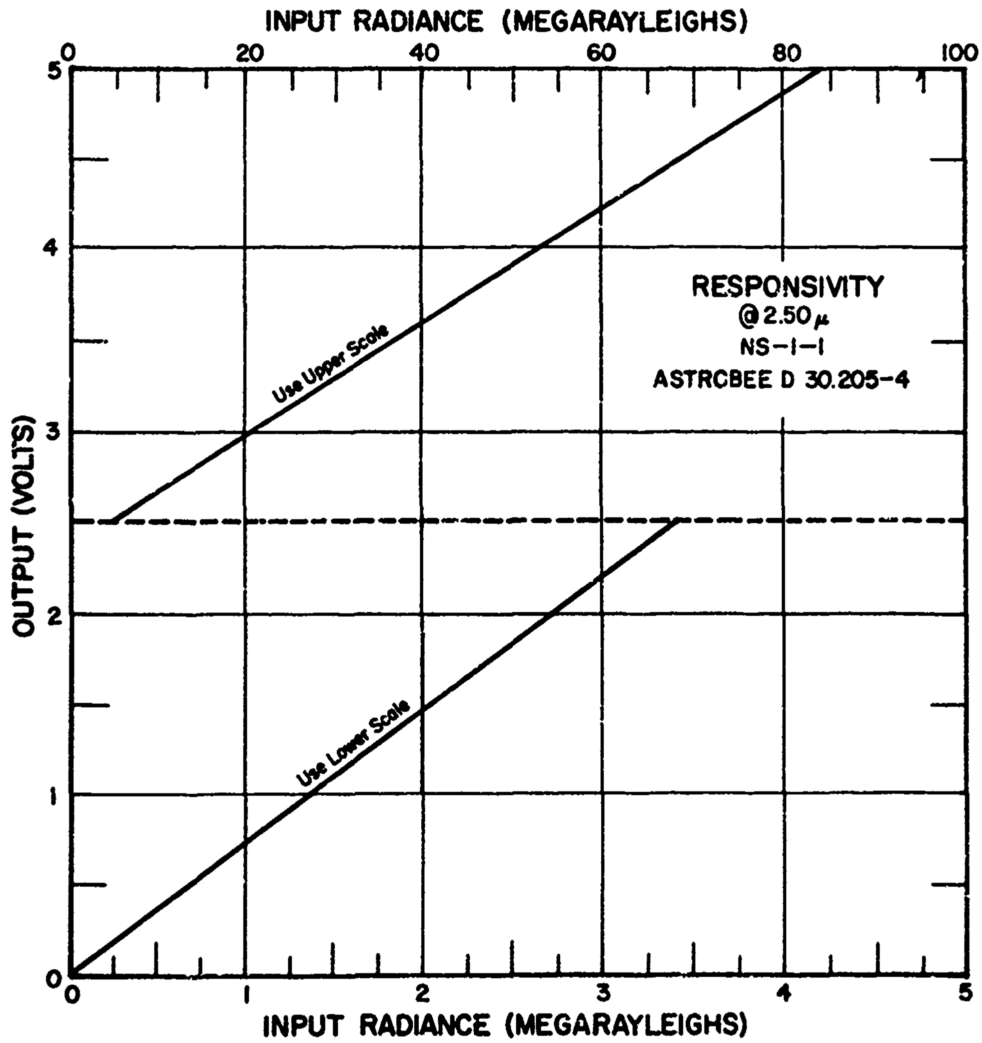

Figure B-5. Responsivity @ 2.50μ---NS-1-1.

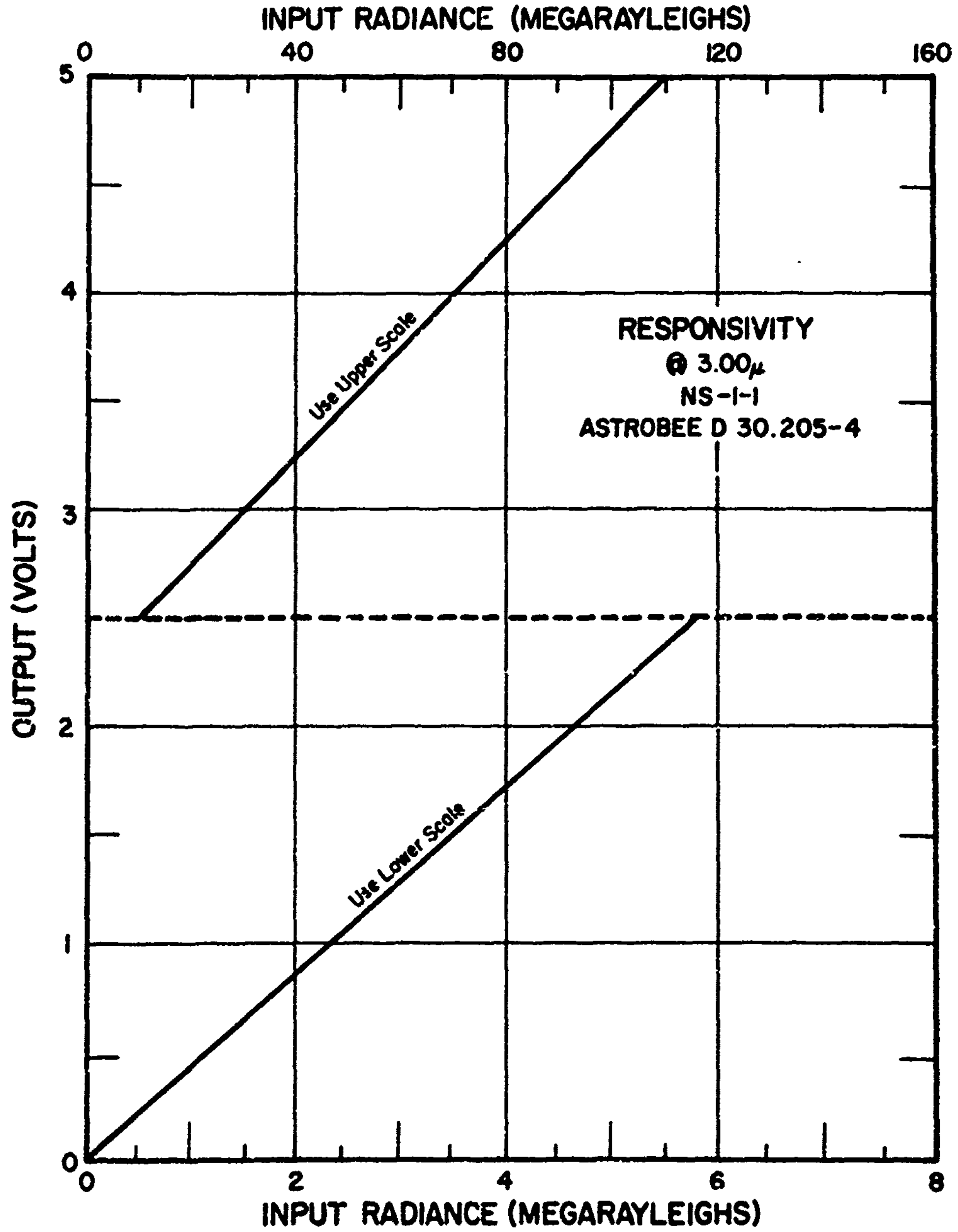

Figure B-6. Responsivity @ 3.00μ---NS-1-1.

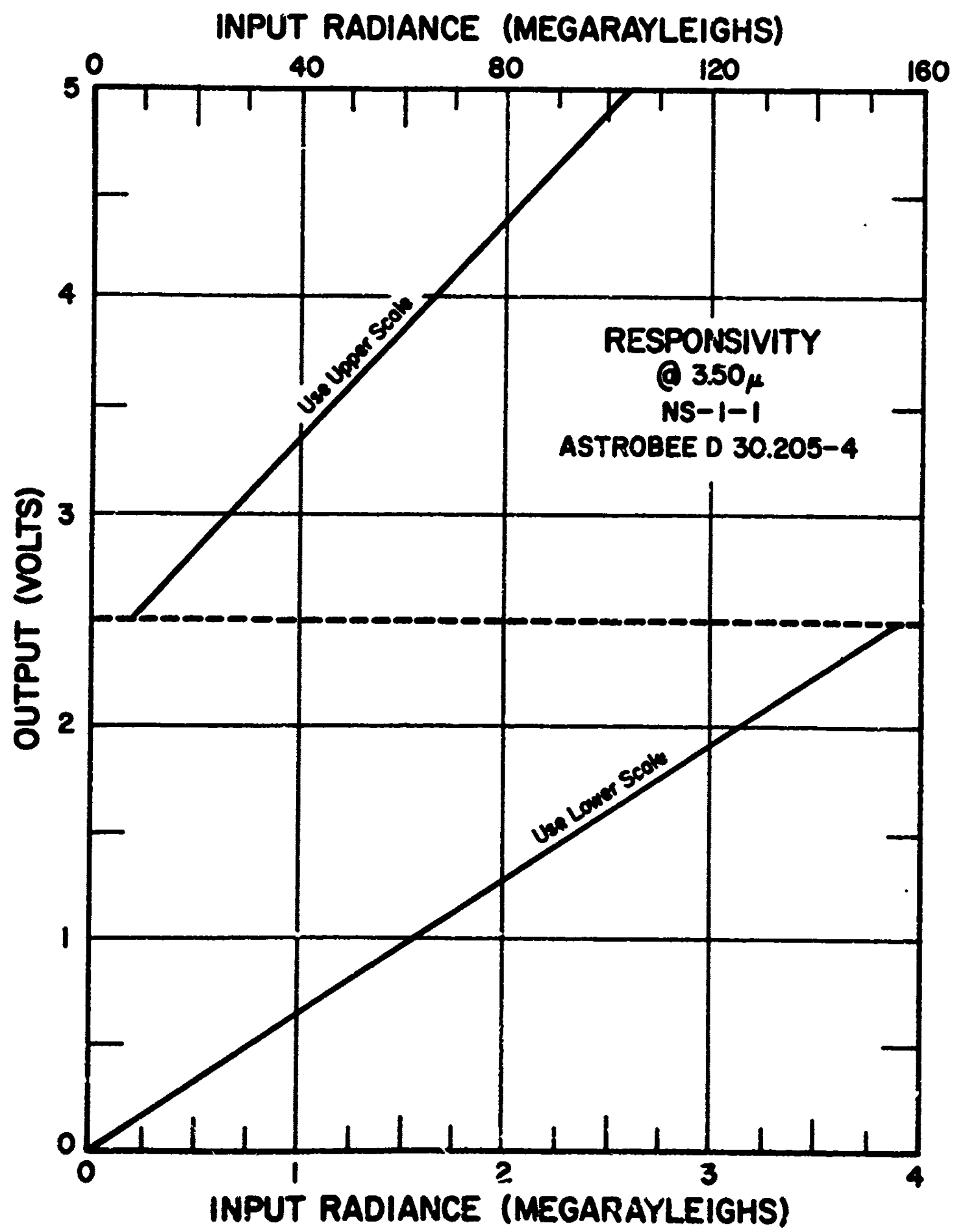

Figure B-7. Responsivity @ 3.50μ---NS-1-1.

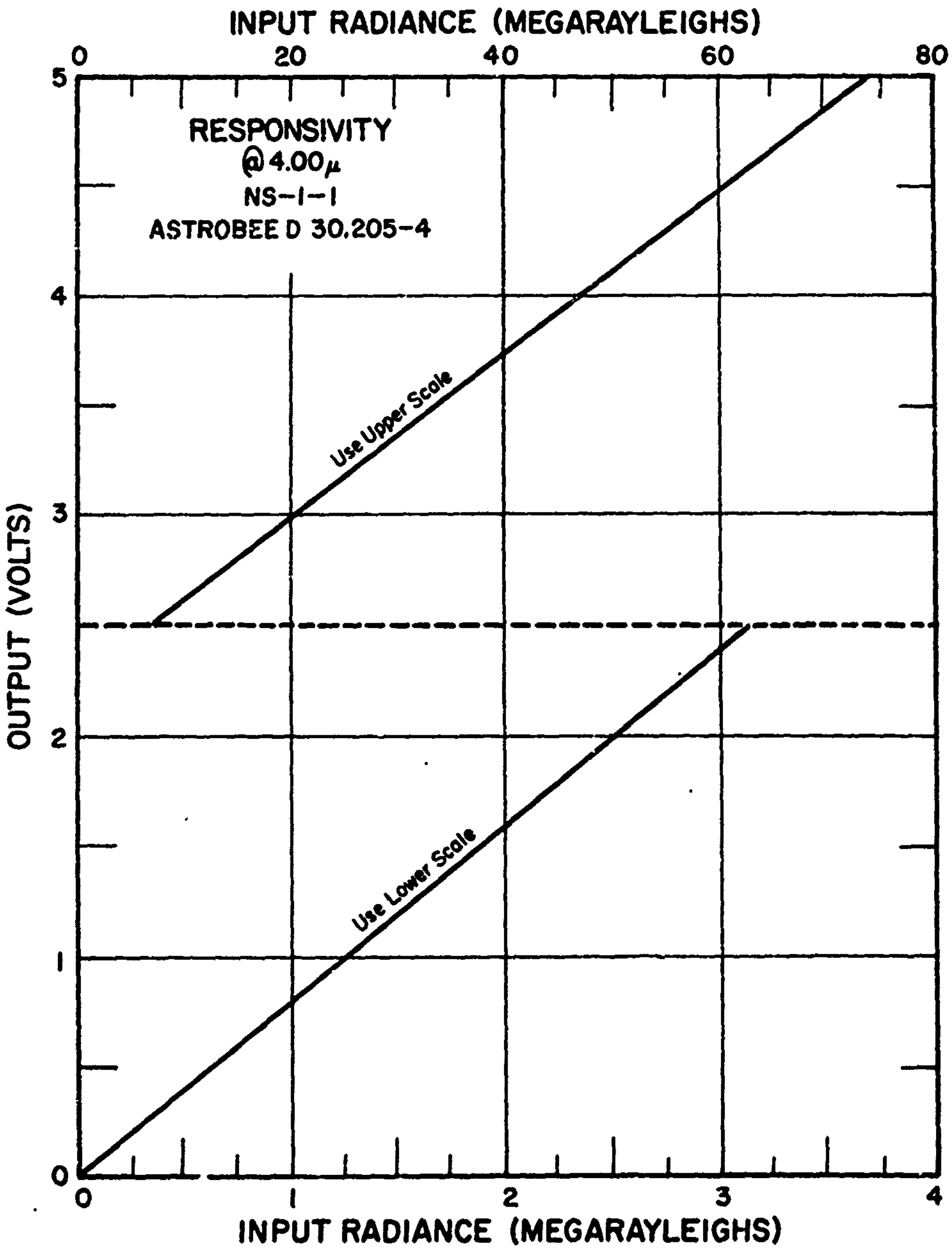

Figure B-8. Responsivity @ 4.00μ---NS-1-1.

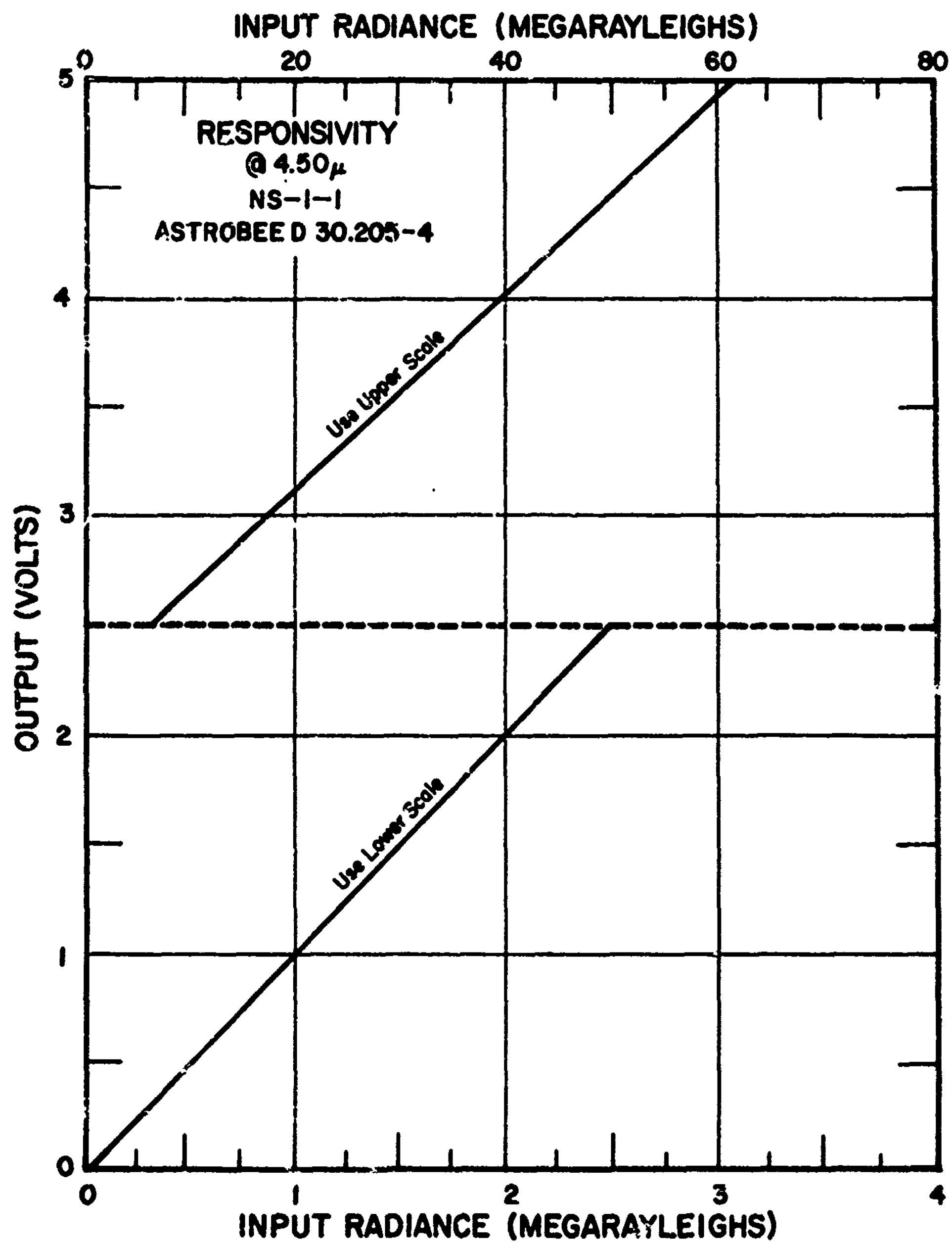

Figure B-9. Responsivity @ 4.50μ---NS-1-1.

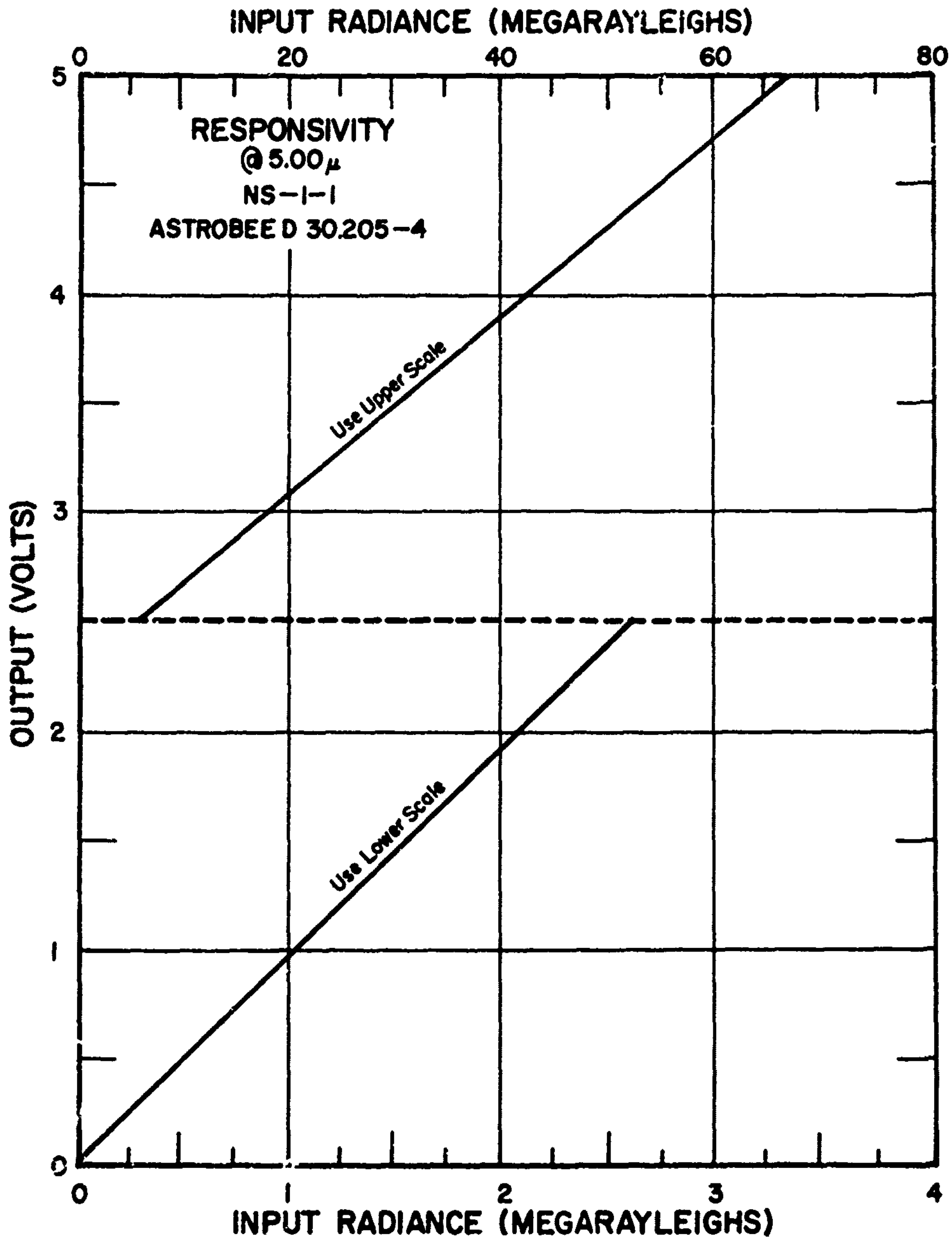

Figure B-10. Responsivity @ 5.00μ---NS-1-1.

APPENDIX C

ASTROBEE D 30.205-3

AND

ASTROBEE D 30.205-4

TRAJECTORY LISTINGS

TABLE C-1

Trajectory Listing - Astrobee D 30.205-3

Launch time - 0214 local, 6 Mar 1972

Time After Launch (sec)	Latitude (Degrees)	Longitude (Degrees)	Altitude (km)	Velocity (km/sec)
28.1	65.1626	147.4535	23.93	1.20
29.1	65.1644	147.4519	25.08	1.19
30.1	65.1662	147.4503	26.21	1.17
31.1	65.1679	147.4488	27.34	1.15
32.1	65.1696	147.4475	28.45	1.14
33.1	65.1712	147.4463	29.55	1.13
34.1	65.1730	147.4451	30.64	1.12
35.1	65.1748	147.4439	31.71	1.10
36.1	65.1765	147.4426	32.77	1.09
37.1	65.1782	147.4413	33.83	1.08
38.1	65.1798	147.4400	34.87	1.07
39.1	65.1815	147.4387	35.90	1.06
40.1	65.1832	147.4374	36.92	1.05
41.1	65.1848	147.4361	37.94	1.04
42.1	65.1864	147.4348	38.94	1.04
43.1	65.1881	147.4335	39.94	1.03
44.1	65.1898	147.4321	40.92	1.02
45.1	65.1915	147.4308	41.90	1.01
46.1	65.1932	147.4294	42.87	1.00
47.1	65.1949	147.4280	43.82	.99
48.1	65.1967	147.4267	44.76	.98
49.1	65.1983	147.4254	45.68	.97
50.1	65.2000	147.4241	46.60	.96
51.1	65.2017	147.4228	47.50	.95
52.1	65.2033	147.4215	48.40	.95
53.1	65.2050	147.4202	49.28	.94
54.1	65.2067	147.4189	50.16	.93
55.1	65.2084	147.4176	51.02	.92
56.1	65.2100	147.4163	51.88	.91
57.1	65.2117	147.4150	52.72	.90
58.1	65.2134	147.4137	53.56	.89
59.1	65.2150	147.4124	54.38	.88
60.1	65.2167	147.4111	55.20	.87
61.1	65.2184	147.4098	56.00	.86
62.1	65.2200	147.4085	56.80	.85
63.1	65.2217	147.4072	57.59	.84
64.1	65.2233	147.4059	58.36	.84
65.1	65.2250	147.4046	59.13	.83
66.1	65.2267	147.4034	59.89	.82
67.1	65.2283	147.4021	60.64	.81
68.1	65.2300	147.4008	61.37	.80
69.1	65.2317	147.3995	62.10	.79

TABLE C-1 (cont.)

Time After Launch (sec)	Latitude (Degrees)	Longitude (Degrees)	Altitude (km)	Velocity (km/sec)
70.1	65.2333	147.3982	62.82	.78
71.1	65.2350	147.3969	63.53	.77
72.1	65.2366	147.3956	64.23	.76
73.1	65.2383	147.3943	64.92	.76
74.1	65.2399	147.3931	65.60	.75
75.1	65.2416	147.3918	66.27	.74
76.1	65.2433	147.3905	66.93	.73
77.1	65.2449	147.3892	67.58	.72
78.1	65.2466	147.3879	68.22	.71
79.1	65.2482	147.3867	68.86	.70
80.1	65.2499	147.3854	69.48	.69
81.1	65.2515	147.3841	70.09	.69
82.1	65.2532	147.3828	70.69	.68
83.1	65.2548	147.3815	71.29	.67
84.1	65.2575	147.3815	71.87	.66
85.1	65.2581	147.3790	72.45	.65
86.1	65.2598	147.3777	73.01	.64
87.1	65.2614	147.3764	73.57	.64
88.1	66.2631	147.3751	74.11	.63
89.1	65.2647	147.3739	74.65	.62
90.1	65.2664	147.3726	75.17	.61
91.1	65.2680	147.3713	75.69	.60
92.1	65.2697	147.3700	76.20	.59
93.1	65.2713	147.3687	76.70	.59
94.1	65.2730	147.3675	77.18	.58
95.1	65.2746	147.3662	77.66	.57
96.1	65.2763	147.3649	78.13	.56
97.1	65.2779	147.3636	78.59	.55
98.1	65.2796	147.3624	79.04	.55
99.1	65.2812	147.3611	79.48	.54
100.1	65.2829	147.3598	79.91	.53
101.1	65.2845	147.3585	80.33	.52
102.1	65.2862	147.3572	80.74	.52
103.1	65.2878	147.3560	81.15	.51
104.1	65.2895	147.3547	81.54	.50
105.1	65.2911	147.3534	81.92	.49
106.1	65.2928	147.3521	82.29	.49
107.1	65.2944	147.3509	82.65	.48
108.1	65.2960	147.3496	83.01	.47
109.1	65.2977	147.3483	83.36	.47
110.1	65.2993	147.3470	83.69	.46
111.1	65.3010	147.3458	84.02	.45
112.1	65.3026	147.3445	84.33	.44
113.1	65.3043	147.3432	84.64	.44
114.1	65.3059	147.3406	84.93	.43

TABLE C-1 (cont.)

Time After Launch (sec)	Latitude (Degrees)	Longitude (Degrees)	Altitude (km)	Velocity (km/sec)
115.1	65.3076	147.3406	85.22	.43
116.1	65.3092	147.3394	85.49	.42
117.1	65.3108	147.3381	85.77	.41
118.1	65.3125	147.3368	86.03	.41
119.1	65.3141	147.3355	86.72	.40
120.1	65.3158	147.3342	86.51	.39
121.1	65.3174	147.3330	86.74	.39
122.1	65.3190	147.3317	86.96	.38
123.1	65.3207	147.3304	87.14	.38
124.1	65.3223	147.3291	87.38	.37
125.1	65.3240	147.3278	87.57	.37
126.1	65.3256	147.3266	87.75	.36
127.1	65.3273	147.3253	87.92	.36
128.1	65.3289	147.3240	88.01	.35
129.1	65.3305	147.3227	88.24	.35
130.1	65.3322	147.3214	88.38	.35
131.1	65.3338	147.3202	88.52	.34
132.1	65.3354	147.3189	88.64	.34
133.1	65.3371	147.3176	88.76	.34
134.1	65.3387	147.3163	88.86	.33
135.1	65.3404	147.3150	88.96	.33
136.1	65.3420	147.3137	89.04	.33
137.1	65.3436	147.3124	89.12	.33
138.1	65.3453	147.3112	89.19	.32
139.1	65.3469	147.3099	89.25	.32
140.1	65.3486	147.3086	89.30	.32
141.1	65.3502	146.3073	89.33	.32
142.1	65.3518	147.3060	89.36	.32
143.1	65.3535	147.3047	89.38	.32
144.1	65.3551	147.3034	89.39	.32
145.1	65.3568	147.3021	89.39	.32
146.1	65.3584	147.3008	89.39	.32
147.1	65.3600	147.2995	89.37	.32
148.1	65.3617	147.2982	89.34	.32
149.1	65.3633	147.2970	89.30	.32
150.1	65.3649	147.2957	89.25	.32
151.1	65.3666	147.2944	89.20	.32
152.1	65.3682	147.2931	89.13	.33
153.1	65.3699	147.2918	89.06	.33
154.1	65.3715	147.2905	88.97	.33
155.1	65.3731	147.2892	88.88	.33
156.1	65.3748	147.2879	88.77	.34
157.1	65.3764	147.2866	88.66	.34
158.1	65.3780	147.2853	88.53	.34
159.1	65.3797	147.2840	88.40	.35

TABLE C-1 (cont.)

Time After Launch (sec)	Latitude (Degrees)	Longitude (Degrees)	Altitude (km)	Velocity (km/sec)
160.1	65.3813	147.2827	88.26	.35
161.1	65.3830	147.2814	88.11	.35
162.1	65.3846	147.2801	87.95	.36
163.1	65.3862	147.2788	87.77	.36
164.1	65.3879	147.2774	87.59	.37
165.1	65.3895	147.2761	87.40	.37
166.1	65.3911	147.2748	87.20	.38
167.1	65.3928	147.2735	86.99	.38
168.1	65.3944	147.2722	86.78	.39
169.1	65.3961	147.2709	86.55	.39
170.1	65.3977	147.2696	86.31	.40
171.1	65.3993	147.2683	86.06	.41
172.1	65.4010	147.2670	85.80	.41
173.1	65.4026	147.2656	85.54	.42
174.1	65.4042	147.2643	85.26	.42
175.1	65.4059	147.2630	84.98	.43
176.1	65.4075	147.2617	84.68	.44
177.1	65.4092	147.2604	84.38	.44
178.1	65.4108	147.2590	84.06	.45
179.1	65.4124	147.2577	83.74	.46
180.1	65.4141	147.2564	83.40	.46
181.1	65.4157	147.2551	83.06	.47
182.1	65.4173	147.2537	82.71	.48
183.1	65.4190	147.2524	82.35	.49
184.1	65.4206	147.2511	81.97	.49
185.1	65.4223	147.2497	81.59	.50
186.1	65.4239	147.2484	81.20	.51
187.1	65.4255	147.2471	80.80	.52
188.1	65.4272	147.2457	80.39	.52
189.1	65.4288	147.2444	79.97	.53
190.1	65.4304	147.2431	79.54	.54
191.1	65.4321	147.2417	79.10	.55
192.1	65.4337	147.2404	78.66	.55
193.1	65.4354	147.2390	78.20	.56
194.1	65.4370	147.2377	77.73	.57
195.1	65.4386	147.2363	77.25	.58
196.1	65.4403	147.2350	76.77	.59
197.1	65.4419	147.2337	76.27	.59
198.1	65.4436	147.2323	75.76	.60
199.1	65.4452	147.2309	75.25	.61
200.1	65.4468	147.2296	74.72	.62
201.1	65.4485	147.2282	74.19	.63
202.1	65.4501	147.2269	73.65	.63
203.1	65.4518	147.2255	73.09	.64
204.1	65.4534	147.2242	72.53	.65

TABLE C-1 (cont.)

Time After Launch (Sec)	Latitude (Degrees)	Longitude (Degrees)	Altitude (km)	Velocity (km/sec)
205.1	65.4550	147.2228	71.96	.66
206.1	65.4567	147.2214	71.37	.67
207.1	65.4583	147.2201	70.78	.68
208.1	65.4600	147.2187	70.18	.69
209.1	65.4616	147.2173	69.57	.69
210.1	65.4633	147.2160	68.95	.70
211.1	65.4649	147.2146	68.32	.71
212.1	65.4665	147.2132	67.68	.72
213.1	65.4682	147.2119	67.03	.73
214.1	65.4698	147.2105	66.37	.74
215.1	65.4715	147.2091	65.70	.75
216.1	65.4731	147.2077	65.02	.75
217.1	65.4748	147.2063	64.33	.76
218.1	65.4764	147.2049	63.64	.77
219.1	65.4780	147.2036	62.93	.78
220.1	65.4797	147.2022	62.21	.79
221.1	65.4813	147.2008	61.49	.80
222.1	65.4830	147.1994	60.75	.81
223.1	65.4846	147.1980	60.00	.82
224.1	65.4863	147.1966	59.25	.82
225.1	65.4879	147.1952	58.48	.83
226.1	65.4896	147.1938	57.71	.84
227.1	65.4912	147.1924	56.93	.85
228.1	65.4928	147.1910	56.13	.86
229.1	65.4945	147.1896	55.33	.87
230.1	65.4961	147.1882	54.52	.88
231.1	65.4978	147.1868	53.70	.89
232.1	65.4994	147.1854	52.86	.90
233.1	65.5011	147.1840	52.02	.90
234.1	65.5027	147.1825	51.17	.91
235.1	65.5044	147.1811	50.31	.92
236.1	65.5060	147.1797	49.44	.93
237.1	65.5077	147.1783	48.56	.94
238.1	65.5093	147.1769	47.68	.95
239.1	65.5110	147.1754	46.78	.96
240.1	65.5126	147.1740	45.87	.97
241.1	65.5142	147.1726	44.96	.97
242.1	65.5159	147.1712	43.10	.98
243.1	65.5175	147.1697	43.10	.99
244.1	65.5192	147.1683	42.15	1.00
245.1	65.5208	147.1669	41.20	1.01
246.1	65.5225	147.1654	40.24	1.02
247.1	65.5241	147.1640	39.27	1.03
248.1	65.5257	147.1626	38.29	1.03
249.1	65.5274	147.1611	37.30	1.04

TABLE C-1 (cont.)

Time After Launch (Sec)	Latitude (Degrees)	Longitude (Degrees)	Altitude (km)	Velocity (km/sec)
250.1	65.5290	147.1597	36.31	1.05
251.1	65.5306	147.1583	35.31	1.06
252.1	65.5323	147.1568	34.30	1.06
253.1	65.5339	147.1554	33.28	1.07
254.1	65.5355	147.1540	32.26	1.07
255.1	65.5371	147.1525	31.23	1.08
256.1	65.5387	147.1511	30.19	1.08
257.1	65.5403	147.1497	29.15	1.09
258.1	65.5419	147.1483	28.11	1.09
259.1	65.5435	147.1469	27.06	1.09
260.1	65.5451	147.1455	26.02	1.09
261.1	65.5466	147.1441	24.97	1.09
262.1	65.5481	147.1427	23.93	1.09
263.1	65.5497	147.1413	22.89	1.08
264.1	65.5512	147.1400	21.86	1.07
265.1	65.5526	147.1387	20.84	1.06
266.1	65.5540	147.1374	19.83	1.05
267.1	65.5554	147.1361	18.83	1.03
268.1	65.5568	147.1349	17.86	1.01
269.1	65.5581	147.1337	16.90	.98
270.1	65.5594	147.1326	15.98	.96
271.1	65.5606	147.1315	15.08	.92
272.1	65.5617	147.1304	14.21	.89
273.1	65.5628	147.1294	13.38	.86
274.1	65.5639	147.1285	12.59	.82
275.1	65.5649	147.1276	11.83	.78
276.1	65.5658	147.1268	11.11	.74
277.1	65.5666	147.1260	10.43	.71
278.1	65.5674	147.1253	9.79	.67
279.1	65.5681	147.1246	9.18	.64
280.1	65.5688	147.1239	8.61	.60
281.1	65.5695	147.1234	8.07	.57
282.1	65.5701	147.1228	7.56	.54
283.1	65.5706	147.1223	7.08	.52

TABLE C-2

Trajectory Listing - Astrobee D 30.205-4

Launch time - 0052 local, 9 Mar 1972

Time After Launch (sec)	Latitude (Degrees)	Longitude (Degrees)	Altitude (km)	Velocity (km/sec)
33.0	65.1889	147.4541	30.43	1.27
34.0	65.1912	147.4530	31.52	1.11
35.0	65.1935	147.4519	32.60	1.10
36.0	65.1957	147.4507	33.67	1.09
37.0	65.1981	147.4495	34.72	1.08
38.0	65.2004	147.4482	35.77	1.07
39.0	65.2026	147.4470	36.81	1.06
40.0	65.2049	147.4457	37.83	1.05
41.0	65.2072	147.4445	38.85	1.04
42.0	65.2096	147.4432	39.85	1.03
43.0	65.2119	147.4420	40.84	1.02
44.0	65.2142	147.4409	41.83	1.01
45.0	65.2165	147.4397	42.80	1.00
46.0	65.2188	147.4386	43.77	.99
47.0	65.2210	147.4374	44.72	.98
48.0	65.2233	147.4363	45.67	.97
49.0	65.2255	147.4351	46.61	.96
50.0	65.2277	146.4340	47.53	.95
51.0	65.2299	147.4329	48.45	.94
52.0	65.2321	147.4317	49.36	.93
53.0	65.2343	147.4307	50.26	.92
54.0	65.2365	147.4296	51.14	.91
55.0	65.2387	147.4285	52.02	.91
56.0	65.2408	147.4274	52.89	.90
57.0	65.2430	147.4264	53.75	.89
58.0	65.2452	147.4253	54.60	.88
59.0	65.2473	147.4242	55.44	.87
60.0	65.2495	147.4232	56.27	.86
61.0	65.2516	147.4222	57.10	.85
62.0	65.2537	147.4211	57.91	.84
63.0	65.2558	147.4201	58.72	.83
64.0	65.2579	147.4191	59.51	.82
65.0	65.2599	147.4181	60.30	.81
66.0	65.2620	147.4172	61.07	.81
67.0	65.2641	147.4162	61.84	.80
68.0	65.2661	147.4152	62.60	.79
69.0	65.2681	147.4143	63.35	.78
70.0	65.2702	147.4133	64.08	.77
71.0	65.2722	147.4124	64.81	.76
72.0	65.2742	147.4114	65.54	.75
73.0	65.2762	147.4105	66.25	.74

TABLE C-2 (cont.)

Time After Launch (sec)	Latitude (Degrees)	Longitude (Degrees)	Altitude (km)	Velocity (km/sec)
74.0	65.2782	147.4096	66.95	.73
75.0	65.2801	147.4087	67.64	.72
76.0	65.2821	147.4078	68.32	.72
77.0	65.2841	147.4068	68.99	.71
78.0	65.2863	147.4057	69.65	.70
79.0	65.2884	147.4047	70.30	.69
80.0	65.2906	147.4036	70.94	.68
81.0	65.2927	147.4025	71.56	.67
82.0	65.2949	147.4015	72.18	.66
83.0	65.2970	147.4004	72.79	.65
84.0	65.2991	147.3994	73.39	.64
85.0	63.3013	147.3983	73.98	.63
86.0	65.3034	147.3972	74.56	.63
87.0	65.3056	147.3962	75.13	.62
88.0	65.3077	147.3951	75.69	.61
89.0	65.3098	147.3941	76.24	.60
90.0	65.3120	147.3930	76.79	.59
91.0	65.3141	147.3919	77.32	.58
92.0	65.3163	147.3909	77.84	.57
93.0	65.3184	147.3898	78.35	.56
94.0	65.3205	147.3888	78.86	.56
95.0	65.3227	147.3877	79.35	.55
96.0	65.3248	147.3866	79.84	.54
97.0	65.3269	147.3856	80.31	.53
98.0	65.3291	147.3845	80.78	.52
99.0	65.3312	147.3835	81.23	.51
100.0	65.3334	147.3824	81.68	.51
101.0	65.3355	147.3814	82.11	.50
102.0	65.3376	147.3803	82.54	.49
103.0	65.3398	147.3792	82.96	.48
104.0	65.3419	147.3782	83.37	.47
105.0	65.3440	147.3771	83.76	.46
106.0	65.3462	147.3761	84.15	.46
107.0	65.3483	147.3750	84.53	.45
108.0	65.3504	147.3739	84.90	.44
109.0	65.3526	147.3729	85.26	.43
110.0	65.3547	147.3718	85.61	.42
111.0	65.3568	147.3708	85.95	.42
112.0	65.3589	147.3697	86.28	.41
113.0	65.3611	147.3686	86.61	.40
114.0	65.3632	147.3676	86.92	.39
115.0	65.3653	147.3665	87.22	.39
116.0	65.3675	147.3654	87.51	.38
117.0	65.3696	147.3644	87.80	.37

TABLE C-2 (cont.)

Time After Launch (sec)	Latitude (Degrees)	Longitude (Degrees)	Altitude (km)	Velocity (km/sec)
118.0	65.3717	147.3633	88.07	.36
119.0	65.3739	147.3622	88.34	.35
120.0	65.3760	147.3612	88.59	.35
121.0	65.3781	147.3601	88.84	.34
122.0	65.3802	147.3591	89.07	.34
123.0	65.3824	147.3580	89.30	.33
124.0	65.3845	147.3569	89.52	.32
125.0	65.3866	147.3559	89.72	.32
126.0	65.3888	147.3548	89.92	.31
127.0	65.3909	147.3537	90.11	.31
128.0	65.3930	147.3527	90.29	.30
129.0	65.3951	147.5316	90.46	.30
130.0	65.3973	147.3505	90.62	.29
131.0	65.3994	147.3494	90.77	.29
132.0	65.4015	147.3484	90.91	.28
133.0	65.4036	147.3473	91.04	.28
134.0	65.4058	147.3462	91.16	.27
135.0	65.4079	147.3452	91.27	.27
136.0	65.4100	147.3441	91.37	.26
137.0	65.4121	147.3430	91.47	.26
138.0	65.4143	147.3419	91.55	.26
139.0	65.4164	147.3409	91.62	.26
140.0	65.4185	147.3398	91.69	.25
141.0	65.4206	147.3387	91.74	.25
142.0	65.4228	147.3376	91.79	.25
143.0	65.4249	147.3365	91.82	.25
144.0	65.4270	147.3355	91.85	.25
145.0	65.4291	147.3344	91.87	.25
146.0	65.4313	147.3333	91.87	.25
147.0	65.4334	147.3322	91.87	.25
148.0	65.4355	147.3311	91.86	.25
149.0	65.4376	147.3301	91.84	.25
150.0	65.4398	147.3290	91.81	.25
151.0	65.4419	147.3279	91.77	.25
152.0	65.4440	147.3268	91.72	.25
153.0	65.4461	147.3257	91.66	.25
154.0	65.4483	147.3246	91.59	.26
155.0	65.4504	147.3235	91.51	.26
156.0	65.4525	147.3224	91.42	.26
157.0	65.4546	147.3213	91.32	.27
158.0	65.4568	177.3203	91.21	.27
159.0	65.4589	147.3192	91.10	.27
160.0	65.4610	147.3181	90.97	.28
161.0	65.4631	147.3170	90.83	.28

TABLE C-2 (cont.)

Time After Launch (sec)	Latitude (Degrees)	Longitude (Degrees)	Altitude (km)	Velocity (km/sec)
162.0	65.4653	147.3159	90.69	.29
163.0	65.4674	147.3148	90.53	.29
164.0	65.4695	147.3137	90.37	.30
165.0	65.4716	147.3126	90.20	.30
166.0	65.4738	147.3115	90.01	.31
167.0	65.4759	147.3104	89.82	.32
163.0	65.4780	147.3093	89.62	.32
169.0	65.4801	147.3082	89.40	.33
170.0	54.4822	147.3071	89.18	.33
171.0	65.4844	147.3060	88.95	.34
172.0	65.4865	147.3048	88.71	.35
173.0	65.4886	147.3037	88.46	.35
174.0	65.4907	147.3026	88.20	.36
175.0	65.4929	147.3015	87.93	.37
176.0	65.4950	147.3004	87.65	.38
177.0	65.4971	147.2993	87.36	.38
178.0	65.4992	147.2982	87.06	.39
179.0	65.5014	147.2971	86.76	.40
180.0	65.5035	147.2959	86.44	.41
181.0	65.5056	147.2948	86.11	.41
182.0	65.5078	147.2937	85.78	.42
183.0	65.5099	147.2926	85.43	.43
184.0	65.5120	147.2914	85.07	.44
185.0	65.5141	147.2903	84.71	.44
186.0	65.5163	147.2892	84.33	.45
187.0	65.5184	147.2881	83.95	.46
188.0	65.5205	147.2869	83.56	.47
189.0	65.5226	147.2858	83.14	.48
190.0	65.5248	147.2847	82.74	.48
191.0	65.5269	147.2835	82.32	.49
192.0	65.5290	147.2824	81.89	.40
193.0	65.5311	147.2813	81.44	.51
194.0	65.5333	147.2801	80.99	.52
195.0	65.5354	147.2790	80.53	.53
196.0	65.5375	147.2778	80.06	.54
197.0	65.5397	147.4767	79.58	.54
198.0	65.5418	147.2755	79.09	.55
199.0	65.5439	147.2744	78.69	.56
200.0	65.5460	147.2732	78.09	.57
201.0	65.5482	147.2721	77.57	.58
202.0	65.5503	147.2709	77.04	.59
203.0	65.5524	147.2698	76.50	.60
204.0	65.5546	147.2686	75.96	.60
205.0	65.5567	147.2675	75.40	.61

TABLE C-2 (cont.)

Time After Launch (sec)	Latitude (Degrees)	Longitude (Degrees)	Altitude (km)	Velocity (km/sec)
206.0	65.5588	147.2663	74.83	.62
207.0	65.5610	147.2651	74.26	.63
208.0	65.5631	147.2641	73.67	.64
209.0	65.5652	147.2628	73.08	.65
210.0	65.5674	147.2616	72.48	.66
211.0	65.5695	147.2065	71.86	.67
212.0	65.5617	147.2593	71.24	.67
213.0	65.5737	147.2581	70.61	.68
214.0	65.5759	147.2570	69.96	.69
215.0	65.5780	147.2558	69.31	.70
216.0	65.5801	147.2546	68.65	.71
217.0	65.5823	147.2543	67.98	.72
218.0	65.5844	147.2522	67.30	.73
219.0	65.5866	147.2511	66.61	.74
220.0	65.5887	147.2499	65.91	.75
221.0	65.5908	147.2487	65.20	.76
222.0	65.5930	147.2475	64.48	.76
223.0	65.5951	147.2463	63.75	.77
224.0	65.5972	147.2451	63.01	.78
225.0	65.5994	147.2439	62.26	.79
226.0	65.6015	147.2427	61.51	.80
227.0	65.6036	147.2415	60.74	.81
228.0	65.6058	147.2403	59.96	.82
229.0	65.6079	147.2391	59.18	.83
230.0	65.6100	147.2379	58.38	.84
231.0	65.6122	147.2367	57.58	.85
232.0	65.6143	147.2355	56.76	.86
233.0	65.6165	147.2343	55.94	.86
234.0	65.6186	147.2330	55.11	.87
235.0	65.6207	147.2318	54.26	.88
236.0	65.6229	147.2306	53.41	.89
237.0	65.6250	147.2294	52.55	.90
238.0	65.6271	147.2282	51.68	.91
239.0	65.6293	147.2269	50.80	.92
240.0	65.6314	147.2257	49.91	.93
241.0	65.6335	147.2245	49.01	.94
242.0	65.6357	147.2233	48.10	.95
243.0	65.6378	147.2220	47.18	.95
244.0	65.6399	147.2208	46.26	.96
245.0	65.6421	147.2196	45.32	.97
246.0	65.6442	147.2183	44.38	.98
247.0	65.6463	147.2171	43.43	.99
248.0	65.6485	147.2158	42.47	1.00
249.0	65.6506	147.2146	41.50	1.00

TABLE C-2 (cont.)

Time After Launch (sec)	Latitude (Degrees)	Longitude (Degrees)	Altitude (km)	Velocity (km/sec)
250.0	65.6527	147.2134	40.52	1.01
251.0	65.6548	147.2121	39.44	1.02
252.0	65.6569	147.2109	38.54	1.03
253.0	65.6569	147.2097	37.54	1.03
254.0	65.6612	147.2084	36.54	1.04
255.0	65.6632	147.2072	35.52	1.04
256.0	65.6653	147.2059	34.50	1.05
257.0	65.6674	147.2047	33.48	1.05
258.0	65.6695	147.2035	32.45	1.06
259.0	65.6715	147.2023	31.42	1.06
260.0	65.6736	147.2011	30.39	1.06
261.0	65.6756	147.1998	29.36	1.06
262.0	65.6776	147.1987	28.33	1.06
263.0	65.6796	147.1975	27.30	1.05
264.0	65.6815	147.1963	26.28	1.04
265.0	65.6835	147.1951	25.26	1.03
266.0	65.6853	147.1940	24.25	1.02
267.0	65.6872	147.1929	23.26	1.01
268.0	65.6890	147.1918	22.28	.99
269.0	65.6907	147.1908	21.33	.97
270.0	65.6924	147.1898	20.39	.94
271.0	65.6940	147.1888	19.48	.91
272.0	65.6956	147.1878	18.60	.88
273.0	65.6970	147.1869	17.76	.85
274.0	65.6984	147.1861	16.94	.81
275.0	65.6998	147.1853	16.17	.77
276.0	65.7010	147.1845	15.43	.73
277.0	65.7022	147.1838	14.73	.69
278.0	65.7032	147.1831	14.07	.65
279.0	65.7042	147.1825	13.44	.62
280.0	65.7052	147.1819	12.86	.58
281.0	65.7060	147.1814	12.30	.54
282.0	65.7068	147.1809	11.79	.51
283.0	65.7076	147.1804	11.30	.48
284.0	65.7082	147.1800	10.84	.45
285.0	65.7089	147.1796	10.41	.42
286.0	65.7094	147.1793	10.00	.40
287.0	65.7100	147.1790	9.62	.38
288.0	65.7104	147.1787	9.25	.36
289.0	65.7109	147.1784	8.91	.34
290.0	65.7113	147.1781	8.58	.32
291.0	65.7117	147.1779	8.27	.31
292.0	65.7120	147.1776	7.97	.29
293.0	65.7124	147.1774	7.69	.28
294.0	65.7127	147.1772	7.42	.27

TABLE C-2 (cont.)

Time After Launch (sec)	Latitude (Degrees)	Longitude (Degrees)	Altitude (km)	Velocity (km/sec)
295.0	65.7129	147.1771	7.16	.26
296.0	65.7132	147.1769	6.90	.25
297.0	65.7134	147.1767	6.66	.24
298.0	65.7137	147.1766	6.42	.23
299.0	65.7139	147.1765	6.20	.23
300.0	65.7141	147.1763	5.98	.22

TABLE C-3

Astrobee D Nosetip Separation Altitudes

Rocket	Separation Altitude
30.205-3	49.10 km
30.205-4	47.19 km